



**Abstract.** Meteorological data from the United Kingdom Meteorological Office (UKMO), produced using a data assimilation system, and the US National Meteorological Center (NMC), produced using an objective analysis procedure, are compared for dynamically active periods during the Arctic and Antarctic winters of 1992. The differences seen during these periods are generally similar to those seen during other winter periods. Both UKMO and NMC analyses capture the large scale evolution of the stratospheric circulation during northern hemisphere (NH) and southern hemisphere (SH) winter. Stronger vertical and horizontal temperature gradients develop in the UKMO than in the NMC data during stratospheric warmings: comparison with satellite measurements with better vertical resolution suggests that the stronger vertical temperature gradients are more realistic. The NH polar vortex is slightly stronger in the UKMO analyses than in the NMC in the middle and upper stratosphere, and mid-stratospheric temperatures are slightly lower. The SH polar vortex as represented in the UKMO analyses is stronger and colder in the mid-stratosphere than its representation in the NMC analyses. The UKMO analyses on occasion exhibit some difficulties in representing cross-polar flow or changes in curvature of the wind field at very high latitudes. In addition to the above study of two wintertime periods, a more detailed comparison of lower stratospheric temperatures is done for all Arctic and Antarctic winter periods since the launch of the Upper Atmosphere Research Satellite. In the NH lower stratosphere during winter, NMC temperatures are consistently lower than UKMO temperatures, and closer to radiosonde temperatures than are UKMO temperatures. Conversely, in the SH lower stratosphere during winter, UKMO temperatures are typically lower than NMC, and are closer to radiosonde temperature observations.

## 1. Introduction

Instruments on board the Upper Atmosphere Research Satellite (UARS) have been measuring stratospheric temperatures, winds, and constituent species since its launch in September 1991. Among the correlative data that aid in interpretation of UARS data are two sets of global meteorological analyses. One is provided by the UK Meteorological Office (UKMO), the other by the US National Meteorological Center (NMC). Both analyses incorporate measurements made by radiosondes and by the NOAA series of polar-orbiting satellites, though the analysis techniques are quite different. The UKMO uses a data assimilation technique to produce daily analyses of geopotential height, temperature and winds [*Swinbank and O'Neill*, 1994a]. The NMC uses an objective analysis scheme to produce daily analyses of temperatures and geopotential heights (from which winds may be computed) [*Gelman et al.*, 1994]. These two datasets are both being widely used to help interpret UARS measurements; it is thus important to determine how consistently they represent the stratospheric circulation. The degree to which the two datasets agree gives an indication of the reliability of both datasets. Where they disagree, it is sometimes possible to relate differences to known shortcomings in the analysis procedures. Understanding the differences between the two datasets will help those who wish to use meteorological data in scientific analyses to determine to what level of detail they may rely on such data.

We begin to address these questions by comparing UKMO and NMC temperatures, geopotential heights, winds, and potential vorticity (PV) calculated from the analyses for dynamically active periods in the northern hemisphere (NH) and southern hemisphere (SH) winters. The periods chosen for detailed consideration are January 1992 in the NH and mid-August to mid-September 1992 in the SH. Dynamically active periods are chosen since differences in the analyses are likely to be most apparent at such times. During January 1992, there was a strong stratospheric warming, which had a lasting impact on the NH stratospheric circulation. The evolution of the stratospheric

circulation during this period was described by *O'Neill et al.* [1994] using UKMO data, and by *Rosier et al.* [1994] using temperatures measured by the Improved Stratospheric And Mesospheric Sounder (ISAMS) on UARS. Certain aspects of the stratospheric circulation in this period were described using NMC analyses by *Manney and Zurek* [1993] and *Newman et al.* [1993].

Several minor warmings disturbed the SH circulation in August 1992; aspects of the stratospheric circulation during this period were described by *Fishbein et al.* [1993] using temperature and ozone data from the Microwave Limb Sounder (MLS) on UARS, by *Manney et al.* [1993] using MLS ozone and NMC analyses, and by *Manney et al.* [1994a] using UKMO analyses.

In addition to understanding the general patterns of differences between the two datasets, many researchers are particularly interested in detailed information on high latitude wintertime lower stratospheric temperatures. These are important in studies of lower stratospheric chemistry and microphysics, including polar stratospheric cloud (PSC) formation, chlorine chemistry and ozone depletion. Because the lower stratospheric temperature retrievals from UARS instruments are not for the most part currently consistently useful for scientific analyses, research in this area is particularly dependent on analyses such as the NMC and UKMO. We therefore include here a section discussing more detailed comparisons of lower stratospheric temperatures, including some discussion of differences between UKMO and NMC analyses during each winter since the UARS launch.

## 2. Data and Analysis

### 2.1. The UKMO assimilation system

The UKMO data assimilation system is a development of the system used to analyze observations for operational weather forecasting, as described by *Lorenc et al.*

[1991]. The stratospheric assimilation system is described in detail by *Swinbank and O'Neill* [1994a]. At the heart of the assimilation system is a global numerical model of the atmosphere extending from the surface to the lower mesosphere, covering the stratosphere with a vertical resolution of about 1.6 km. The horizontal resolution of the model is  $2.5^\circ$  latitude by  $3.75^\circ$  longitude.

As the model is integrated forward, its fields are adjusted towards the observed data at each time step. The weight given to each observation depends on the difference between the model and observation time, so observations are given most weight at the exact time they are valid. The repeated insertion ensures that the model is gradually adjusted to new observations, so a measure of dynamical balance is maintained. It also ensures that slowly varying modes of the model are preferred; these generally correspond to the atmospheric motions that we wish to study. The weights given to the observations also take into account the expected accuracy of the observations, so that the evolving state of the numerical model is a realistic representation of the state of the atmosphere to within the assumed errors.

Before being assimilated into the model, observations are put through a quality control stage. Observed values are checked against values from a numerical forecast from an earlier analysis. On the basis of expected errors in the observation and forecast, a statistical check is carried out to assess the possibility that each observation is grossly in error. Any erroneous data are not passed to the assimilation. After the assimilation has been completed, a dataset of statistics on data and model accuracy is compiled.

Each day, the numerical model is run for 24 hours in data assimilation mode. At the end of this period (at 12 GMT daily) the model writes out a set of analyzed fields interpolated to the standard UARS pressure levels from 1000 hPa to 0.316 hPa. The horizontal resolution of the fields is the same as in the numerical model. These analyses are supplied to the UARS Central Data Handling Facility (CDHF).

## 2.2. The NMC analysis system

The NMC objective analysis system is a modified Cressman analysis for pressure levels from 70 hPa to 0.4 hPa [*Finger et al.*, 1965; *Gelman and Nagatani*, 1977]. A number of changes to the analysis and data used are documented by *Gelman et al.* [1986] and *Finger et al.* [1993]. The NMC analyses in the NH are based exclusively on data from the NOAA series TIROS Operational Vertical Sounders (TOVS) in the upper stratosphere [*Gelman et al.*, 1994]. In the NH lower stratosphere (10 hPa and below), rawinsonde data are used [*Gelman et al.*, 1994; *Finger et al.*, 1965]. Analyses at and below 100 hPa are from the tropospheric analysis and forecast cycle [*Derber et al.*, 1991]. In the SH, exclusively satellite data are used from 70 hPa to 0.4 hPa [*Gelman et al.*, 1994].

The current NMC analysis method is described in more detail by *Gelman et al.* [1994]. TOVS information from the NOAA 11 satellite constitute the data used for upper stratospheric analyses at 5, 2, 1 and 0.4 hPa in the northern hemisphere, and throughout the stratosphere in the southern hemisphere. Temperature profiles are provided to NMC as layer mean temperatures between standard pressure levels. Geopotential heights are derived using these to calculate thicknesses via the hypsometric equation. The NMC 100 hPa height analysis is used as a base height to obtain heights above 100 hPa. Temperatures are derived by log-linear interpolation between the given TOVS layer mean temperatures. These heights and temperatures are then analyzed on a 65 by 65 polar stereographic grid. The NMC fields are produced each day for 12 GMT, using 12 hours of TOVS data from 6 to 18 GMT to provide full global coverage. In the NH, 70, 50, 30 and 10 hPa rawinsonde data are analyzed using a successive approximation scheme, with the first guess being the analysis of TOVS derived temperature and geopotential height. Thus, in the NH, the NMC temperatures are closely fitted to radiosonde temperatures where such measurements are available.

*Finger et al.* [1993] compared NMC upper stratospheric temperature analyses with

rocketsonde and lidar data, and suggested a set of offsets that should be subtracted from NMC temperatures at and above 5 hPa. The measurements used in *Pfister et al.*'s [1993] comparison were all in the NH, and predominantly at middle latitudes; the suggested corrections are based on comparisons during a number of different seasons and meteorological conditions. *Fishbein et al.* [1995] showed that differences between NMC temperatures (with the suggested biases subtracted) and temperatures from MLS in the upper stratosphere were greater at high latitudes than at middle and low latitudes during both NH and SH winter. *Dudhia and Livesey* [1995] showed similar results when comparing “corrected” NMC temperatures with ISAMS data. As noted by *Pfister et al.* [1993], the biases between NMC and rocketsonde and lidar data are strongly affected by dynamical variations, and the corrections are of greatest value for studies of relatively long term trends and climatology. For the comparisons we present here of short term evolution during dynamically active periods, the suggested biases are not subtracted from the upper stratospheric fields - the comparisons shown are for NMC and UKMO analyses as they are distributed on the CDHF.

The NMC data are provided to the CDHF on the 65 by 65 polar stereographic grids for each hemisphere, on 18 standard pressure levels, from 1000 to 0.4 hPa. For this study, NMC fields are interpolated using a cubic spline to the standard UARS pressure levels, and to a  $4^\circ$  latitude by  $5^\circ$  longitude horizontal grid.

### 2.3 Analysis

The archive of NMC data does not include wind fields above 50 hPa. All the NMC wind fields used in this study are calculated, on the NMC polar stereographic grids, from geopotential heights using a form of the primitive equations that neglects the vertical advection and time tendency terms [*Randel*, 1987; *Newman et al.*, 1989]. The resulting wind fields, together with other NMC analysis fields, are interpolated to a  $4^\circ$  latitude by  $5^\circ$  longitude grid, similar to grids typically used for plotting UARS data.

UKMO wind fields are produced as an integral part of the data assimilation. They are determined both by actual wind observations (primarily in the troposphere and lower stratosphere), and by wind information inferred from temperature measurements in a dynamically consistent manner by the assimilation procedure. Before any UKMO fields are plotted, they are first interpolated to a polar stereographic grid like that used for the NMC data, and then to the  $4^\circ$  latitude by  $5^\circ$  longitude grid.

A number of derived products are calculated and archived on a daily basis from both UKMO and NMC data. These include potential temperature ( $\theta$ ), zonal and meridional winds, and Rossby-Ertel potential vorticity (PV),

$$PV = -g(\zeta_\theta + f) \cdot \frac{\partial \theta}{\partial p},$$

where  $\zeta_\theta$  is the component of relative vorticity orthogonal to the  $\theta$  surface, and  $f = 2\Omega \sin(\text{latitude})$  is the planetary vorticity. Potential vorticity is calculated on a polar stereographic grid from both UKMO and NMC data, using an algorithm based on that given by *Newman et al.* [1989]. All products are interpolated to a  $4^\circ$  latitude by  $5^\circ$  longitude grid before plotting. For quantities such as PV, which are useful when displayed on an isentropic surface, isentropic surfaces were defined that lie near the UARS pressure levels, and products are routinely produced on these levels.

In this paper, we show what we consider to be the best product derived from each dataset. Hence, winds shown for the UKMO data are those produced by the assimilation model. To illustrate some of the limitations of the wind calculation used for NMC data, Fig. 1 shows the difference between winds calculated from the UKMO geopotential heights and winds produced by the UKMO assimilation system. The plot shows the differences in zonal mean wind on 11 Jan 1992, near the beginning of the January 1992 stratospheric warming. The largest differences are confined to the tropics, where the wind calculation is not expected to do well [*Randel, 1987*], but where the UKMO analyses have been shown to produce realistic structures, such as the quasi-biennial



oscillation and semi-annual oscillation [*Swinbank and O'Neill, 1994b*]. For the polar regions, which are the focus of this study, the approximate winds are in good agreement with the winds from the assimilation procedure, except at the very highest latitudes above about 5 hPa, where the UKMO assimilation model occasionally has problems with cross-polar flow (see below). Figure 2 shows 840 K PV maps produced from UKMO data using the calculated winds, and the winds from the assimilation procedure. Differences are very small, and at relatively small scales, giving the field produced using the calculated winds a somewhat more “lumpy” appearance than that produced using the winds from the assimilation model. Closer comparison of these fields shows no significant differences in the larger scale characteristics, for instance, the maximum PV gradients along the vortex edge are virtually identical. This suggests that, away from the equator, we can reasonably compare fields from NMC with winds derived by the procedure described above with fields derived using the UKMO assimilation model winds.

### 3. Northern Hemisphere, January 1992

#### 3.1. Time Evolution of Temperatures and Winds

Fig. 3 shows time series of zonal mean temperatures as a function of latitude at 10 hPa for January 1992, from UKMO (Fig. 3a) and NMC (Fig. 3b) analyses, and the difference between the two (Fig. 3c). A strong stratospheric warming occurred during the period 8 to 12 January: at 10 hPa zonal-mean temperatures increased by about 35 K in three days. Although high-latitude NMC temperatures are slightly higher overall through the period, the two analyses give much the same picture of the temperature variations during the warming. There are, however, two short periods when there are significant temperature differences between the analyses. The first is during the buildup of the warming, when strong horizontal and vertical temperature gradients develop.

NMC temperatures are up to 12 K higher than UKMO temperatures in the zonal mean. This difference corresponds to a slightly delayed onset of strong warming in the UKMO analyses. During the onset of the warming, a strong cross-polar jet developed in the stratosphere [e.g., *O'Neill et al.*, 1994], leading to increased numerical errors in the UKMO grid-point model at polar latitudes. The second period of large zonal-mean temperature differences is towards the end of the warming on 18 January, when NMC temperatures are up to 14 K higher than UKMO temperatures in the zonal mean. Small errors of position of the cross-polar jet and associated strong temperature gradients can appear as large differences in zonal-mean temperatures at high latitudes. South of about  $65^{\circ}\text{N}$ , zonal-mean temperature differences are almost always less than 2 K.

A similar plot of zonal-mean temperatures at 46 hPa from UKMO and NMC analyses, and the difference between the two is shown in Fig. 4. Temperature difference equatorward of  $65^{\circ}\text{N}$  are less than about 1 K. Poleward of this, UKMO zonal mean temperatures tend to be higher than those from NMC by 1 to 2 K. The exceptions to this are at extremely high latitudes at the onset of the warming, which is earlier in NMC than in UKMO analyses, and around 19-21 January, after the peak of the warming. Lower stratospheric temperatures will be discussed in more detail in Section 5.

In the upper stratosphere, at 1 hPa, Fig. 5 shows that NMC temperatures are systematically lower than UKMO temperatures. This bias is larger at middle and low latitudes (4 to 6 K), and for short periods at high latitudes when there is cross-polar flow. *Pinger et al.* [1993] reported a cold bias of 6.2 K in 1 hPa NH NMC temperatures. This agrees well with the bias between NMC and UKMO temperatures at middle and low latitudes. As was the case at 10 hPa, the onset of the warming is slightly later in the UKMO data, leading to the positive difference on about 10 January.

The following figures compare UKMO and NMC zonal mean winds during January 1992. Fig. 6 shows 10 hPa zonal mean zonal winds from NMC and UKMO analyses, and the difference between the two. Before and after the warming, maximum UKMO

winds are slightly stronger than winds calculated from NMC analyses. The stratospheric warming is accompanied by rapid deceleration of the zonal-mean westerly winds at middle and high latitudes. The evolution of zonal-mean winds is qualitatively similar in the two analyses, but there are significant differences of up to  $15 \text{ ms}^{-1}$  in zonal wind speed at high latitudes, consistent with the large differences in polar temperatures noted above. After about 20 January, the zonal mean jet in the UKMO analysis is centered at higher latitude than in the NMC analysis. The method used to compute winds from the NMC analyses has not introduced a noticeable bias in the winds derived from NMC temperatures.

In the lower stratosphere, at 46 hPa, we see in Fig. 7 that, equatorward of about  $65^\circ\text{N}$ , wind differences are generally less than  $5 \text{ ms}^{-1}$ . Noticeable differences are seen only near the pole at the onset of the warming, and in late January, when, as in the middle and upper stratosphere, the jet maximum is closer to the pole in the UKMO than in the NMC analyses.

Fig. 8 shows zonal mean winds at 1 hPa, and the difference between UKMO and NMC zonal-mean wind at that level. Weaker NMC winds from about  $30^\circ$  to  $70^\circ\text{N}$  beginning around 10 January are consistent with the earlier onset of the warming in the NMC analyses. UKMO winds are stronger near the pole from approximately 12 to 16 January, as easterly winds in the UKMO data become about  $10 \text{ ms}^{-1}$  stronger at the peak of the warming than do NMC winds. Elsewhere in this period, differences between UKMO and NMC winds are small except at very high latitudes, indicating that the bias seen in NMC temperatures at this level does not have a strong impact on the calculation of winds from NMC analyses.

The time evolution of zonal-mean temperatures at a function of height at  $68^\circ\text{N}$ , and the difference between UKMO and NMC analyses, is shown in Fig. 9. The strong warming between approximately 8 and 18 January is preceded by a weak warming that affects only levels above 10 hPa. Higher NMC temperatures at the beginning of January

suggest that the onset of this weak warming is also earlier in NMC than in UKMO analyses. During most of the strong warming, in particular before about 13 January, the UKMO analysis shows stronger vertical temperature gradients than the NMC analysis. The increase in temperature at the highest levels is more rapid in the UKMO than in the NMC analysis, with the UKMO field obtaining maximum temperatures on 12 January, and the NMC on 14 January. A cold bias in NMC analyses is apparent above about 2 hPa. Below about 20 hPa, there may be a slight cold bias of up to approximately 1 K of NMC with respect to UKMO temperature, as was apparent in Fig. 4. Differences in similar vertical sections of zonal-mean winds (not shown) are consistent with the results previously shown. The main differences between UKMO and NMC analyses are, as noted in the horizontal sections, that both easterly and westerly winds are stronger in the UKMO analyses in the upper stratosphere, and that the onset of the warmings occurs slightly earlier in the NMC than in the UKMO analyses.

### 3.2. Synoptic Fields

The synoptic evolution of the stratospheric circulation in January 1992 has been described by several authors, including *Naujokat et al.* [1992], *Manney and Zurek* [1993], *O'Neill et al.* [1994], and *Farman et al.* [1994]. An anticyclone, the “Aleutian high”, which is a climatological feature in the NH mid-winter stratosphere, was present before the onset of the warming [e.g., *Rosier et al.*, 1994], with a strong cross-polar jet between the cyclone and anticyclone. The Aleutian high intensifies during the warming, temperatures rise sharply in the jet stream between the two vortices, and the cyclone weakens [e.g., *O'Neill et al.*, 1994]. As was apparent in the differences between UKMO and NMC analyses shown in the previous section, largest differences between the two datasets are seen during the warming, before its peak.

Fig. 10 shows UKMO and NMC 10 hPa geopotential height and temperature on 11 January, in the midst of the warming, and the difference between NMC and UKMO

geopotential heights and temperatures. The most apparent difference between UKMO and NMC geopotential heights is in the position of the vortex, which is shifted slightly eastward in the UKMO with respect to the NMC, leading to differences up to about 500 m on the eastern and western poleward flanks of the jet. As expected, largest temperature differences are in the region of strong temperature gradients, between the cyclone and anticyclone, with stronger temperatures gradients in the UKMO data leading to differences up to 25 K locally. The pattern of temperature differences on 11 January is typical of most days during this period; however, there are some days during this period, run with an earlier version of the assimilation system [*Swinbank and O'Neill, 1994a*] when significant problems with cross-polar flow in the model give rise to unrealistic patterns in the UKMO analyses. Temperature differences away from the region of strong gradients typically lie in the range -5 K to +5 K. Differences between NMC and UKMO geopotential height and temperatures fields on other days during the period studied are typically less than on 11 January, but the patterns are similar, with maximum differences in regions of strong temperature gradients. In general, the maximum horizontal temperature gradients in the UKMO fields are somewhat stronger than those in the NMC, as is seen on 11 January 1992.

A qualitatively similar situation is seen at 1 hPa (Fig. 11). At this level, the intensification of the Aleutian high is more pronounced. Comparison with Fig. 10 shows that a westward and equatorward tilt of the vortex with height has developed [e.g., *Farman et al., 1994*], as commonly happens during stratospheric warmings [e.g., *Fairlie et al., 1990*; *Manney et al., 1994b*]. As at 10 hPa, the vortex in the UKMO analysis is shifted eastward with respect to the NMC, giving rise to maximum geopotential height differences up to approximately 800 m. The 1 hPa UKMO temperature fields are somewhat noisy, likely due to the proximity of the model top [*Swinbank and O'Neill, 1994a*]. The maximum temperature differences are up to 10 K, in the region of strong temperature gradients between the cyclone and anticyclone, on 13 January. Away from

the polar region of strong temperatures gradients, NMC temperatures are generally lower than UKMO, a reflection of the known cold bias in NMC at that level.

As noted above, a strong baroclinic zone in temperature forms during the warming [e.g., *Farman et al.*, 1994], with the warmest air at 1 hPa (Fig. 11) overlying the coldest air at 10 hPa (Fig. 10). In Fig. 12, we show a cross-section through this baroclinic zone in UKMO and NMC analyses. Fig. 12 comprises a cross-section of temperature along the 60°N latitude circle from NMC and UKMO, and the difference between the two, on 11 January. A strong baroclinic zone is apparent from about 30 to 2 hPa. Vertical temperature gradients on 11 January between 10 and 3 hPa in the NMC field are  $\sim 7$  K/km; those in the UKMO field are  $\sim 10$  K/km. Closer examination of vertical temperatures gradients along other sections and on other days during the period indicates that the UKMO fields usually have stronger vertical and horizontal temperature gradients in the region of strongest temperature gradients.

A common concern with meteorological analyses such as these is their ability to resolve sharp vertical structures such as baroclinic zones in temperature. Because most of the stratospheric data involved in these analyses is from operational sounders with very broad weighting function peaks, and only a few channels in the regions of interest, the vertical resolution of these datasets is considered to be poor. The use of an assimilation model such as in the UKMO analyses may allow the model to predict smaller vertical structures. Analyses of limb-sounding satellite data with better vertical resolution from ISAMS [e.g., *Rosier et al.*, 1994] suggests that actual vertical temperature gradients are, in fact, sharper than those in either of the analyses shown here.

Many studies use PV to examine the evolution of the stratospheric polar vortex. Because of the differentiation involved in calculating PV, differences in the fields are magnified in the calculated PV. Figure 13 shows PV maps on 11 January calculated from UKMO and NMC analyses, at 465 K (near 50 hPa, lower stratosphere), 840 K

(near 10 hPa, middle stratosphere), and 1450 K (near 2 hPa, upper stratosphere). Throughout the period studied, differences in the lower stratosphere are in points of detail, i.e., small differences in the shape of the vortex, the local strength of the PV gradients, and the continuity of tongues of PV pulled off the vortex (e.g., near 40°N and 0° to 90°W in Fig. 13). In the middle stratosphere, PV gradients around the polar vortex are slightly stronger in the UKMO than in the NMC fields. Differences in the position of the vortex seen in Fig. 10 in the geopotential height fields are not as apparent here. The NMC PV fields tend to have a “scalloped” appearance, especially at low latitudes. This probably results from the effects of the NMC analysis on data from satellite orbit tracks that are, at low latitudes, widely spaced. The PV calculation also magnifies small differences that, in the geopotential height and temperature fields, may not be immediately visible - note that the difference fields shown in Figs. 10 and 11 do show significant structure on the scale of these “lumps”, away from the regions of largest differences. The wind calculation also tends to give slightly “lumpier” fields, as discussed in Section 2.3. At 1450 K, in the upper stratosphere, maximum PV gradients are noticeably higher in the UKMO than in the NMC fields, and maximum PV values are also higher; this makes the vortex appear larger in the UKMO than in the NMC field. The “scaloping” in the low latitude NMC PV is again apparent, but indications of material drawn off the vortex and around to near 90°E can be seen in both NMC and UKMO fields. PV calculated from the UKMO analyses is generally found to get noisier at higher levels, as is apparent in the 1450 K UKMO PV field; these small scale features are not thought to represent real atmospheric structure.

## 4. Southern Hemisphere, August-September 1992

### 4.1. Time Evolution of Temperatures and Winds

*Fishbein et al.* [1993] showed the evolution of MLS temperatures during a series

of minor warmings in late August and early September 1992 in the SH stratosphere. The synoptic evolution of the flow during this time was briefly shown by *Manney et al.* [1993], and by *Randel et al.* [1993], both using PV derived from NMC analyses. A series of three minor warmings occurred, with the strongest wave activity around 5 Sep 1992. These warmings were strongest in the middle and upper stratosphere, and did not have a large effect on the lower stratosphere [*Fishbein et al.*, 1993; *Manney et al.*, 1993], as is typical of minor warmings in the SH.

Figure 14 shows time series of zonal mean temperatures as a function of latitude at 10 hPa, for 15 August through 14 September 1992, from UKMO and NMC analyses, and the difference between the two. Temperatures near the pole increase by about 15 K in 3 days starting on about 2 September. As was the case in the NH, the temperature increase begins slightly earlier in the NMC than in the UKMO data. The increase is also slower in the NMC data. As can be seen quite clearly in the difference plot, 10 hPa temperatures are higher in overall in the NMC than in the UKMO data. The difference increases dramatically at high latitudes; poleward of  $72^\circ$ , NMC temperatures are more than 6 K warmer through most of this time interval. Although temperature gradients were also stronger in the UKMO data in the NH, the overall warm bias of the NMC with respect to the UKMO was small there, no more than 2 K. This difference in zonal mean temperatures was also noted by *Swinbank and O'Neill* [1994a]. The difference is larger during the strong minor warming, indicating that this event is having less of an effect on the UKMO than on the NMC fields.

Similar time series of 46 hPa temperatures are shown in Figure 15. A slight increase in temperatures around 5 September is the only noticeable effect of the warming here. The timing of this at high latitudes appears similar in both fields, although the warming near  $40^\circ\text{S}$  begins earlier in the UKMO field. As at 10 hPa, the most noticeable difference in the fields is that UKMO temperatures are lower than NMC temperatures, especially at high latitudes, where differences are from 0.5 to 1.5 K before the warming, and as



large as 3.5 K during the warming. There is thus less warming in the UKMO zonal mean temperatures at high latitudes as a result of wave activity at this time; however, at about 50°S, there is more warming in the UKMO than in the NMC field.

At 1 hPa (not shown), differences between NMC and UKMO fields are similar to those reported for the NH. NMC temperatures are overall approximately 3-5 K lower than UKMO temperatures at high latitudes, a bias slightly smaller than that seen by *Finger et al.* [1993] for NH NMC temperatures with respect to rocketsondes. The time evolution of temperature is similar in both fields, with slight differences near the pole. The warming is much weaker at 1 hPa than in the mid-stratosphere.

The stronger latitudinal temperature gradients in the UKMO data result in a stronger polar night jet, as shown in Figure 16 at 10 hPa. Maximum zonal mean winds in the UKMO are 8 to 10 m/s higher than in the NMC, and the location of the jet maximum in the UKMO data is slightly poleward of that in the NMC data. The effect of the minor warming can be seen around 4 September, when maximum winds decrease by about 20 - 30 m/s. Zonal mean winds throughout the stratosphere (not shown) have very similar differences between UKMO and NMC. At each level the jet in the UKMO data is poleward of and stronger than that in the NMC data.

Figure 17 shows time series of zonal mean UKMO and NMC temperatures as a function of pressure at 68°S. The development of the warming can be seen to be somewhat slower in the NMC than in the UKMO field, as was apparent in the 10 hPa temperatures (Fig. 14). From approximately 70 to 3 hPa, UKMO temperatures are lower than NMC, with the largest differences of about 6 K near 10 hPa. Above 3 hPa, the cold bias in the NMC data is apparent. A similar section of zonal mean winds is shown in Figure 18. As noted above, UKMO winds are stronger than NMC at all levels. Although the winds do not decrease as much in the UKMO data, the decrease that occurs around 4 September is more rapid than the corresponding increase in the NMC data, especially in the upper stratosphere.

## 4.2 Synoptic Fields

Figure 19 compares 10 hPa geopotential heights and temperatures from NMC and UKMO data on 4 September, near the peak of the warming. NMC temperatures are substantially warmer almost everywhere, with a strong dipole pattern in the difference field centered near 70°S, 70°E, where UKMO temperature gradients are stronger. Gradients around the vortex are stronger in the UKMO geopotential height field than in NMC, with the largest differences collocated with the large temperature differences. The generally positive differences poleward of 60° and negative differences equatorward are indicative of the stronger polar vortex in the UKMO fields. All these differences are typical of the differences on any day between UKMO and NMC fields, but the magnitudes of the differences are larger during this minor warming. Figure 20 compares geopotential heights and temperatures on the same day at 1 hPa. At this level, a difference in position of the vortex between UKMO and NMC data is apparent, leading to a strong dipole pattern in the geopotential height difference field. Largest temperature differences are again in the region of strong temperature gradients. A cold bias in NMC is again apparent in the generally negative temperature difference field.

As noted by *Vishbein et al.* [1993], a substantial baroclinic zone forms in the temperature field at the time of the minor warming. Figure 21 shows a latitude/pressure section of UKMO and NMC temperatures around the 60°S latitude circle, and the difference between the two fields. Between approximately 10 and 3 hPa, the NMC fields have maximum vertical temperature gradients of  $\sim 4.5$  K/km, while the UKMO gradients are  $\sim 5.5$  K/km. MLS temperatures, although currently only retrieved with a vertical spacing of about 5 km, have even sharper vertical temperature gradients at this time [*Vishbein et al.*, 1993], suggesting that the true vertical temperature gradients are in fact at least as strong as any of those shown here.

Figure 22 shows PV maps at 465, 840 and 1450 K, on 4 September. As suggested by the previous discussion, the vortex is stronger in the UKMO than in the NMC field

at each level, with most obvious differences at 840 K. At 840 K, the vortex in UKMO data is noticeably more symmetric, consistent with the weaker effect of the warming seen the previous figures. At 1450 K, however, the anticyclonic circulation is stronger in the UKMO than in the NMC data, so that the vortex, although slightly stronger, is not more symmetric. The “scaloped” pattern appears at low latitudes in the NMC PV, as noted in the northern hemisphere. Both UKMO and NMC fields show long tongues of material being stripped off the vortex edge at 840 and 1450 K.

## 5. Lower Stratospheric Temperature Differences

Some biases between NMC and UKMO lower stratospheric temperatures were noted in the zonal means shown above. Many studies of lower stratospheric chemistry and microphysics depend critically on lower stratospheric temperatures. In many cases, analyses such as the UKMO and NMC are the only global (or hemispheric) temperature datasets available in the lower stratosphere, as temperatures from most of the limb-sounding UARS instruments are not, at present, adequately retrieved at these levels (ISAMS temperatures are considered useful in the lower stratosphere, but are available only for a very limited time period [*Dudhia and Livesey, 1995*]). We take a closer look here at differences between NMC and UKMO lower stratospheric temperatures during the winters since the launch of UARS.

Fig. 23 shows the difference (NMC-UKMO) between NMC and UKMO high latitude minimum daily temperatures on the 465 K ( $\sim 50$  hPa, a level that has been the focus of many studies of lower stratospheric dynamics and chemistry) isentropic surface for December through March in each of the NH winters when both datasets are available. The minimum temperatures are for the region with  $PV \geq 0.25 \times 10^{-4} \text{ K m}^2 \text{ kg}^{-1} \text{ s}^{-1}$ , an approximate definition of the edge of the polar vortex during winter. Noted on each panel is the average difference over the period shown. The period December through March covers essentially all of the times when temperatures less than or near type I PSC

formation temperatures have been observed [e.g., Zurek *et al.*, 1995]. Although most of the individual daily differences are within the combined uncertainty in the UKMO and NMC lower stratospheric temperatures [Gelman *et al.*, 1994; Swinbank and O'Neill, 1994a], the differences are by no means random. Through most of the winters, the NMC temperatures are lower than the UKMO, with most of the individual days' differences falling between 1 and 3 K. Two notable exceptions to this are in late December and early January 1992, and in mid-January 1994. These are both times of particularly strong wave activity in the NH - the latter part of the 1992 period has been discussed above, and the January 1994 period immediately follows a strong warming [e.g., Manney *et al.*, 1994a].

In December 1991 and January 1992, a number of adjustments were made to the UKMO assimilation procedure [Swinbank and O'Neill, 1994a]; although these mainly affected the upper stratosphere, some changes in a diagnostic as sensitive as this one in the lower stratosphere may have taken place. During the relatively quiet and cold winters of 1992-93 and 1994-95 [e.g., Zurek *et al.*, 1995], there are few days when UKMO temperatures are as low as NMC temperatures. Higher temperatures in the UKMO analyses are generally consistent with there being somewhat stronger wave activity in the UKMO analyses. Newman *et al.* [1993] showed that for December 1991 through February 1992, the NMC lower stratospheric minimum temperatures were very close to those from radiosondes, except on a few of the coldest days when radiosonde minimum temperatures were 1 to 2 K lower. As was seen in Fig. 8, the region where UKMO temperatures are typically higher than NMC temperatures in the NH is confined to the lower stratosphere, below about 22 hPa; above this, UKMO temperatures are slightly colder in general than NMC, as discussed above.

We have compared both UKMO and NMC analyses with temperatures from radiosonde observations in the lower stratosphere for selected days during the unusually cold 1994-95 winter. In order to compare the ability of each analysis scheme to represent

the coldest temperatures in the lower stratosphere, we present statistics showing how well each analysis fits the radiosonde data when the observed temperatures is less than 200 K. Table 1 summarizes the comparisons for pressures near 50 hPa, and latitudes from 60° to 76°N. Average and rms differences between UKMO and radiosonde temperatures, and between NMC and radiosonde temperatures are given. When considering only observed temperatures less than 200 K, both NMC and UKMO are significantly higher than the radiosondes. This indicates that neither analysis system is completely successful in capturing the coldest observed temperatures.

The above analysis, however, does not give a statistically fair measure of the actual biases between the radiosonde observations and analyses, since it does not include cases when the analyzed temperatures were very cold, and the observed temperatures were less cold. Table 1 also shows the equivalent comparisons between analyzed and radiosonde temperatures for all observations near 50 hPa, to give a more complete picture of the biases and rms differences. In cases where the bias indicated is not statistically significant at the “ $2\sigma$ ” level, the numbers for average bias are italicized. The table shows that the NMC values are close to the radiosonde values in the northern hemisphere, while the UKMO values tend to be higher.

Fig. 24 shows the temperature differences as a function of pressure, a subset of which were used to calculate the  $T < 200$  K differences in Table 1, for 14-15 January 1995 and 28-30 January 1995. What is most apparent in the 14-15 January case is the scatter of both NMC and UKMO temperatures about the radiosonde values. Fig 24b, for 28-30 January is an example of a time when there are the largest differences between minimum UKMO and NMC values (Fig. 23); Fig. 24b indicates that, at levels above approximately 70 hPa, both UKMO and NMC are warmer than radiosondes, but with more of the UKMO comparisons showing a warm bias, and a distinct increase in the UKMO bias with increasing altitude. 28-30 January is during a strong stratospheric warming, and thus is a period which is particularly difficult for the analyses to fit.

Since the NMC NH analyses rely so heavily on fitting to radiosonde measurements where they are available, while the UKMO analysis more equally weights satellite and radiosonde temperatures, it is perhaps not surprising that NMC temperatures are closer to radiosonde temperatures in the NH lower stratosphere than UKMO temperatures, or that the UKMO bias increases with height, as the number of radiosonde measurements used in their analyses decreases.

Fig. 25 shows a plot similar to Fig. 23, but for May through September in the three SH winters for which both datasets are available. As was noted above for August 1992 zonal means (Figs. 15 and 17), the UKMO minimum lower stratospheric temperatures are nearly always lower than NMC temperatures in the SH late winter. UKMO temperatures also appear to usually be lower than NMC during May. In the middle of the winter, NMC and UKMO temperatures show no clear bias, except for a brief period in July 1992, when NMC temperatures are lower. During the period in July 1992, the NMC temperatures drop several degrees over a few days, whereas the UKMO temperatures drop only slightly; the reason for this decrease is not immediately apparent. *Massie et al.* [1994] compared both UKMO and NMC temperatures with radiosondes in the SH during August 1992, and found that UKMO temperatures were closer to radiosondes. *Gelman and Newman* [1988] found that NMC temperatures in August and September 1987 were generally higher than radiosonde measured temperatures at the south pole, near the area of minimum temperatures, at 30 and 50 hPa, but did not show an obvious bias at stations where temperatures were warmer.

Table 2 summarizes comparisons between NMC and UKMO temperatures and radiosondes in the SH for periods during each month of the 1993 winter. As in Table 1, we show rms and average differences for measurements between 34 and 56 hPa, and 60° and 76°S, for radiosonde measurements with  $T < 200$  K, and for all radiosonde measurements in the pressure and latitude range. Both UKMO and NMC biases are small (although most are still significant at the “ $2\sigma$ ” level) during the May, June

and July periods studied. The UKMO analyses during June and July, and during May when measurements at all temperatures are included, are on the average colder than radiosondes, while the NMC analyses are warmer throughout the winter. During August and September, while the UKMO biases remain small, NMC temperatures are substantially warmer than radiosondes, by about 2 K on the average. Fig. 26 shows a plot of differences versus pressure for the measurements used to get the  $T < 200$  K values in Table 2, for 11-19 Aug and 11-19 Sep 1993. The NMC values show an increasing warm bias with increasing altitude during both periods. The UKMO analyses show a similar increasing warm bias with height during 11-19 August, but it is not as strong as in the NMC analyses.

As noted in Section 2, one significant difference between the two analysis systems is that radiosondes are not used in the SH in the NMC lower stratospheric analyses, whereas they are used in the UKMO procedure. Since the satellite measurements used in both analyses are measured over a broad layer, it is not surprising that the UKMO temperatures are closer to radiosondes. However, in the northern hemisphere, the NMC analyses procedure fits the radiosondes more closely than the UKMO because it gives more weight to the radiosonde observations. What is not immediately clear is the cause of the apparent seasonal pattern of the differences between UKMO and NMC analyses (Fig. 25, Table 2). Based on the Table 2 values for all temperatures, there does not appear to be an obvious difference throughout the period in the number of radiosonde measurements available. It is likely that a cold bias in the UKMO assimilation model, possibly attributable to the radiation scheme, may nudge the UKMO analyses towards more rapid cooling in early winter, and slower warming in late winter, than what would be reflected in the purely satellite based NMC SH analyses. It is also possible that the differences are larger because the early and late winter periods are more dynamically active; however, 1993 was the least dynamically active of the three winters throughout, but does not show noticeably smaller differences in Fig. 26.

## 6. Discussion anti Summary

Both the UK Meteorological Office and National Meteorological Center analyses are now available for the four northern winters and three southern winters, since the launch of the UARS satellite. We have compared in some detail the stratospheric circulation represented in those two meteorological data sets, for a dynamically active winter period in each hemisphere.

Many of the differences noted for the periods studied in detail are typical of differences during other wintertime periods. During all northern hemisphere warmings that have been examined, the horizontal and vertical temperature gradients along the edge of the vortex are stronger in the UKMO than in the NMC analyses, as was shown for January 1992. Comparisons with high vertical resolution satellite temperatures suggest that the steeper temperature gradients in the UKMO fields are more realistic (although they still underestimate the real gradients in the atmosphere). The assimilation model used in the UKMO analyses is free to simulate smaller scale structures than those represented in the satellite observations, while the vertical interpolation procedure used for layer-mean temperatures in the NMC analysis probably introduces additional smoothing.

The UKMO grid-point model used for the assimilation at times has problems representing strong cross-polar flow. As was noted in section 3, such problems were particularly severe in the analyses for some days in January 1992. Several adjustments were made to the assimilation parameters around this time [*Swinbank and O'Neill, 1994a*], which helped lessen the severity of such problems. The January 11 analysis shown above (Figs 10-13) was run a few months behind real time, with an updated version of the assimilation model. Some days in and before January 1992, run with earlier versions of the model show unrealistic structure in the fields at high latitudes due to these problems. The 13 January 10 hPa temperature field shown in Fig. 27 is an example of one of the poorer fields; note the unrealistically strong gradients at very high



latitudes near  $90^\circ\text{E}$ . In examining stratospheric warmings in succeeding winters, when there was also strong cross-polar flow, we have not identified any other problems of the same severity.

During relatively undisturbed periods in the northern hemisphere winter similar patterns of difference are seen, although the differences are generally smaller. Fig. 28 shows a time-series for mid-December 1994 to mid-January 1995 of differences between NMC and UKMO 10 hPa zonal mean temperatures and winds. This was an unusually quiet period in the NH winter [e.g. *Zurek et al.*, 1995]. As was found during undisturbed periods in the 1991-92 winter, high latitude UKMO temperatures are up to a few degrees colder than NMC temperatures, and high latitude UKMO winds are up to about 10 m/s stronger than winds calculated from the NMC analyses. These patterns are similar to those seen in the quieter SH middle stratosphere (e.g. Figs 14 and 16), although the NH differences are rather less.

The differences between middle and upper stratospheric winds and temperatures in the southern hemisphere, as described in section 4 for August and September 1992, are typical of SH winters. The pattern of differences in zonal mean winds and temperatures, for all SH winters examined, are very similar to those shown in Figs. 14 through 18. During less active periods the magnitudes of the differences tend to be smaller; for example the maximum differences in 10 hPa zonal mean temperatures was about 6 K in late July 1993 (as opposed to about 10 K in September 1992), and maximum zonal mean wind differences were about 8 m/s (as opposed to about 12 m/s).

During the southern hemisphere winter, it is not uncommon for the curvature of the wind field at high latitudes in the middle and upper stratosphere to be such that the PV gradient changes sign there. When this is the case, the UKMO fields sometimes show unrealistic looking structures in winds and PV at high latitudes. An example of this problem is shown in Fig. 29, which depicts 840 K PV maps from the UKMO and NMC analyses for 5 July 1993. This is probably again related to details of the polar filtering

and representation of cross-polar flow in the UKMO grid-point model. This type of problem is also reflected in the high latitude zonal mean wind field. The representation of PV gradients at high latitudes could be important to dynamical studies such as stability modeling, where results may depend critically on the curvature of the wind field.

In a more general comparison of PV fields, we have found that the two analyses give similar results in the lower stratosphere. The differences are mainly in the small scales, which to some extent have been masked by the interpolation procedures used in this study. The relatively small scale details would not be expected to have a large impact on many studies of dynamics and transport in this region. At higher altitudes unrealistic small scale structure increases in the UKMO PV fields; in the upper stratosphere, the estimated error in the analyzed temperatures is larger, and the increased noise reflects greater uncertainty in the stability term in the calculation of the PV fields.

The polar vortex in the upper stratosphere frequently appears larger and stronger in the UKMO analyses. In the northern hemisphere mid- stratosphere, the UKMO temperatures are slightly lower than NMC in the zonal mean at high latitudes. In the southern hemisphere somewhat larger differences are found, leading to a significantly larger stronger SH stratospheric vortex in the UKMO analyses. Above about 5 hPa, the cold bias in the NMC temperatures [*Finger et al.*, 1993] results in lower NMC than UKMO temperatures. For some dynamical studies the differences between the UKMO and NMC analyses may not materially affect the results; both sets of analyses capture the qualitative features of the large scale motions, and show similar patterns of the evolution of the circulation. However, the differences in temperature and strength of the polar vortex could have a noticeable impact on quantitative studies of stratospheric processes, particularly in the southern hemisphere. For example, there could be a significant impact on studies of transport, especially with regard to the isolation of the vortex, which depends critically on the strength of the polar night jet, and the PV

gradients. There will also be a significant impact on the calculation of radiative heating rates, which depend critically on temperature.

We have also noted small differences in the timing of stratospheric warmings, as pointed out for January 1992 and August/September 1992. Some of these differences probably result from the different way in which observations taken throughout the day are used in the two analysis procedures. While the NMC system simply groups together all observations from a 12 hour period centred on the analysis time, the UKMO system treats the observations asynchronously, varying the weight given to each observation with model time-step. During particularly active periods, when significant changes to the stratospheric circulation can occur during one day, these effects may be important.

Because detailed quantitative knowledge of lower stratospheric temperatures is so important to chemical and microphysical studies of ozone depletion, we have presented a more detailed comparison of those data with radiosonde observations. The results show that NMC lower stratospheric temperatures are generally lower than UKMO temperatures in the northern hemisphere, and in better agreement with radiosonde observations. Conversely, in the southern hemisphere the UKMO temperatures are lower and closer to the radiosonde observations. These overall differences result from the fact that the NMC analyses are fitted very closely to radiosondes in the northern hemisphere, while they do not use radiosondes at all in the southern hemisphere lower stratosphere. In contrast, the UKMO analyses give more equal weighting to radiosonde and satellite observations in both hemispheres. The study also shows that neither analysis system captures the very lowest observed temperatures; the analyses generally have a warm bias compared to radiosonde observations less than 200K. One reason for this bias is the smoothing introduced by the use of satellite soundings with poor vertical resolution, and possibly by the analysis procedures themselves. The exception to this finding is that, at times during early winter in the SH, the UKMO analyses show a small negative bias. This could be related to the influence of a cold bias in the UKMO

assimilation model.

In this study we have focussed on the extratropical wintertime. Although further study of different seasons would be illuminating, we would expect the differences between UKMO and NMC analyses to be smaller in summer, due to the quieter dynamical situation. A study of differences in the tropics would also be informative, although it is beyond the scope of this paper. A number of additional concerns arise at low latitudes, in particular the difficulties of obtaining realistic analyzed winds close to the equator.

## 7. Conclusions

We have examined in detail selected periods in northern and southern hemisphere winters, to highlight the main differences between the UKMO and NMC stratospheric analyses which are provided as correlative data for the UARS project. In general, we have found that there is broad agreement between the two analysis data sets. Both sets of analyses provide a good meteorological framework to describe the overall characteristics and evolution of the stratospheric circulation and to help in the interpretation of measurements from UARS.

For detailed studies, users of both UKMO and NMC analysis data sets should be aware of their different characteristics, which are summarized in Section 6. In many cases, we have been able to relate the differences in the analyses to particular shortcomings in one or the other of the analysis systems. In other cases, there is little independent evidence to distinguish which of the UKMO and NMC analyses is more correct. In such cases it is all the more important to know the typical magnitudes and patterns of differences. These differences can often be taken as an indication of the uncertainty of the analyses, which should be taken into account when using either data set for studies of the stratospheric circulation.

**Acknowledgments.** Thanks to the NMC and UKMO personnel who contribute to making available these analyses; in particular, thanks to M. Bailey, P. Connery, D. Podd and N. Roberts for helping to develop and run the UKMO assimilation system. Thanks to T. Luu for data management at JPL; to P. A. Newman for supplying routines that were adapted to calculate PV; to E. F. Fishbein, L. Froidevaux and M. L. Santee for helpful discussions. The work at the Jet Propulsion Laboratory, California Institute of Technology is part of a UARS theoretical investigation and was carried out under contract with the National Aeronautics and Space Administration. The stratospheric analysis work at the UKMO is supported by the European Commission under contract 1V5V-C"J94-0441. The research at the National Center for Atmospheric Research (NCAR) is supported by the NASA UARS program under contract S-10782-C. NCAR is sponsored by the National Science Foundation.

## References

- D(11)(1, J.C., 1). F. Parrish, and S. J. Lord, The new global operational analysis system at the National Meteorological Center, *Weather and Forecasting*, **6**, 535-5171 1991.
- Dudhia, A., and N. J. Livesey, Validation of temperature measurements from the Improved Stratospheric and Mesospheric Sounder, *J. Geophys. Res.*, submitted, 1995.
- Fairlie, '1'. 1). A., M. Fisher, and A. O'Neill, The development of narrow baroclinic zones and other small-scale structure in the stratosphere during simulated major warmings, *Q. J. R. Meteorol. Soc.*, **116**, 287-315, 1990.
- Farman, J. C., A. O'Neill, and R. Swinbank, The dynamics of the Arctic polar vortex during the EASOE campaign, *Geophys. Res. Lett.*, **21**, 1195-1198, 1994.
- Finger, F. G., M. E. Gelman, J. J. Wild, M. L. Chanin, A. Hauchecorne, and A. J. Miller, Evaluation of NMC upper-stratospheric temperature analyses using rocketsonde and lidar data, *Bull. Am. Meteorol. Soc.*, **74**, 789-799, 1993.
- Finger, F. G., H. M. Woolf, and C. E. Anderson, A method for objective analysis of stratospheric constant pressure charts, *Mon. Weather Rev.*, **93**, 619-638, 1965.
- Fishbein, E. F., L. S. Elson, L. Froidevaux, G. L. Manney, W. G. Read, J. W. Waters, and R. W. Zurek, MLS observations of stratospheric waves in temperature and ozone during the 1992 southern winter, *Geophys. Res. Lett.*, **20**, 1255-1258, 1993.
- Fishbein, E. F., et al., Validation of UARS MLS temperature and pressure measurements, *J. Geophys. Res.*, submitted, 1995.
- Gelman, M. E., and R. M. Nagatani, Objective analyses of height and temperature at the 5-, 2-, and 0.4-mb levels using meteorological rocketsonde and satellite radiation data, *Space Weather (11) (11)*, **XVII**, 117-122, 1977.
- Gelman, M. E., A. J. Miller, K. W. Johnson and R. M. Nagatani, Detection of long term trends in global stratospheric temperature from NMC analyses derived from NOAA satellite data, *Adv. Space Res.*, **6**, No. 10, 17-26, 1986.
- Gelman, M. E., A. J. Miller, R. M. Nagatani, and C. S. Long, Use of UARS data in the NOAA stratospheric monitoring program, *Adv. Space Res.*, **14**, No. 9, 21-31, 1992.

- Lorenc, A. C., R. S. Bell, and B. McPherson, The meteorological office analysis correction data assimilation scheme, *Q. J. R. Meteorol. Soc.*, **117**, 59-89, 1991.
- Manney, G. I., and R. W. Zurek, Interhemispheric comparison of the development of the stratospheric polar vortex during fall: A 3-dimensional perspective for 1991-1992, *Geophys. Res. Lett.*, **20**, 1275-1278, 1993.
- Manney, G. I., L. Froidevaux, J. W. Waters, L. S. Elson, E. F. Fishbein, R. W. Zurek, R. S. Harwood, and W. A. Lahoz, The evolution of ozone observed by UARS MLS in the 1992 late winter southern polar vortex, *Geophys. Res. Lett.*, **20**, 1279-1282, 1993.
- Manney, G. I., R. W. Zurek, A. O'Neill, and R. Swinbank, On the motion of air through the stratospheric polar vortex, *J. Atmos. Sci.*, **51**, 2973-2994, 1994a.
- Manney, G. I., J. D. Farrara, and C. R. Mechoso, Simulations of the February 1979 stratospheric sudden warming: Model comparisons and three-dimensional evolution, *Mon. Weather Rev.*, **122**, 1115-1140, 1994b.
- Massie, S. T., P. L. Bailey, J. C. Gille, E. C. Lee, J. L. Mergenthaler, A. E. Roche, J. B. Kume (T), E. F. Fishbein, J. W. Waters, and W. A. Lahoz, Spectral signatures of polar stratospheric clouds and sulfate aerosols, *J. Atmos. Sci.*, **51**, 3027-3044, 1994.
- Naujokat, B., K. Petzoldt, K. Labitzke, R. Lenschow, B. Rajewski, M. Wiesner, and R.-C. Wohlfart, The stratospheric winter 1991/92: The winter of the European Arctic Stratospheric Ozone Experiment, *Beil. zur Berliner Wetterkarte*, **SO 18/92**, 1992.
- Newman, P. A., L. R. Lait, M. R. Schoeberl, R. M. Nagatani, and A. J. Krueger, Meteorological Atlas of the Northern Hemisphere Lower Stratosphere for January and February 1989-1991 During the Airborne Arctic Stratospheric Expedition, NASA Tech. Memo. **4145**, 185 pp, 1989.
- Newman, P. A., L. R. Lait, M. R. Schoeberl, E. R. Nash, K. Kelly, J. W. Fahey, R. Nagatani, J. Toohey, L. Avallone, J. Anderson, Stratospheric meteorological conditions in the Arctic polar vortex, 1991 to 1992, *Science*, **261**, 1143-1147, 1993.
- O'Neill, A., W. L. Grose, V. D. Pope, H. MacLean, and R. Swinbank, Evolution of the stratosphere during northern winter 1991/92 as diagnosed from U.K. Meteorological Office analyses, *J. Atmos. Sci.*, **51**, 2800-2817, 1994.

- Randel, W. J., The evaluation of winds from geopotential height data in the stratosphere, *J. Atmos. Sci.*, *44*, 3097-3120, 1987.
- Randel, W. J., J. C. Gille, A. E. Roche, J. B. Kumer, J. L. Mergenthaler, J. W. Waters, E. F. Fishbein, and W. A. Lahoz, Stratospheric transport from the tropics to middle latitudes by planetary-wave mixing, *Nature*, *365*, 533-535, 1993.
- Rosier, S. M., B. N. Lawrence, D. G. Andrews, and F. W. Taylor, Dynamical evolution of the northern stratosphere in early winter 1991/92, as observed by the Improved Stratospheric and Mesospheric Sounder, *J. Atmos. Sci.*, *51*, 2783-2799, 1994.
- Swinbank, I., and A. O'Neill, A Stratosphere-troposphere data assimilation system, *Mon. Weather Rev.*, *122*, 686-702, 1994a.
- Swinbank, I., and A. O'Neill, Quasi-biennial and semi-annual oscillations in equatorial wind fields constructed by data assimilation, *Geophys. Res. Lett.*, *21*, 2099-2102, 1994b.
- Zurek, R. W., G. L. Manney, M. E. Gelman, A. J. Miller, and R. Nagatani, Interannual variability of the North Polar vortex in lower stratosphere during the UARS mission, *Geophys. Res. Lett.*, submitted, 1995.



**Figure 1.** Difference ( $\text{m s}^{-1}$ ) in zonal mean winds calculated from UKMO geopotential heights, and from the UKMO assimilation (Calculated - Assimilation, see text), on 11 Jan 1992. Contour interval is  $2 \text{ m s}^{-1}$ , with dashed lines indicating negative values.

**Figure 2.**  $540 \text{ K NII PV}$  calculated from (a) UKMO winds on 11 Jan 1992, and (b) winds derived from UKMO geopotential heights on 11 Jan 1992. Contour interval is  $1 \times 10^{-4} \text{ K m}^2 \text{ kg}^{-1} \text{ s}^{-1}$ , with shading between  $4$  and  $5 \times 10^{-4} \text{ K m}^2 \text{ kg}^{-1} \text{ s}^{-1}$ . Projection is orthographic, with  $0^\circ$  longitude at the bottom of the plots,  $90^\circ\text{E}$  to the right, and  $30^\circ$  and  $60^\circ \text{ N}$  latitude circles as dashed lines.

**Figure 3.** Time-series of UKMO and NMC zonal mean  $1 \text{ hPa}$  temperatures (K) for January 1992, and the difference between the two (NMC - UKMO). Temperature contour interval is  $5 \text{ K}$ , with  $235$  to  $240 \text{ K}$  shaded. Difference contour interval is  $3 \text{ K}$ , with dashed lines indicating negative values.

**Figure 4.** As in Fig. 3, but at  $46 \text{ hPa}$ . Temperature contour interval is  $2.5 \text{ K}$ , with  $197.5$  to  $200 \text{ K}$  shaded. Difference contour interval is  $1 \text{ K}$ .

**Figure 5.** As in Fig. 3, but at  $1 \text{ hPa}$ . Temperature contour interval is  $3 \text{ K}$ , with  $255$  to  $257 \text{ K}$  shaded. Difference contour interval is  $2 \text{ K}$ .

**Figure 6.** As in Fig. 3, but for zonal mean wind ( $\text{m s}^{-1}$ ). Wind contour interval is  $5 \text{ m s}^{-1}$ , with  $25$  to  $30 \text{ m s}^{-1}$  shaded. Difference contour interval is  $4 \text{ m s}^{-1}$ .

**Figure 7.** As in Fig. 6, but for  $46 \text{ hPa}$ . Wind contour interval is  $3 \text{ m s}^{-1}$ , with  $21$  to  $24 \text{ m s}^{-1}$  shaded. Difference contour interval is  $1.5 \text{ m s}^{-1}$ .

**Figure 8.** As in Fig. 6, but for  $1 \text{ hPa}$ . Wind contour interval is  $10 \text{ m s}^{-1}$ , with  $30$  to  $40 \text{ m s}^{-1}$  shaded. Difference contour interval is  $5 \text{ m s}^{-1}$ .

**Figure 9.** As in Fig. 3, but a pressure time section at  $68^\circ\text{N}$ . Temperature contour interval is  $5 \text{ K}$ , with  $235$  to  $240 \text{ K}$  shaded. Difference contour interval is  $2 \text{ K}$ .

**Figure 10.** 10 hPa N11 geopotential height (colors, km) and temperature (contours, K) from UKMO (top) and NMC (middle) on 11 Jan 1992, and the difference (NMC - UKMO, bottom) between the two geopotential height fields (colors, km) and the two temperature fields (contours, K). Layout is as in Fig. 2. Temperature contour interval is 5 K; temperature difference contour interval is 5 K, with dashed lines indicating negative values. Color bars give geopotential height contours.

**Figure 11.** As in Fig. 10, but at 1 hPa. Temperature contour interval is 5 K; temperature difference contour interval is 5 K. Color bars give geopotential height contours.

**Figure 12.** UKMO (top) and NMC (middle) temperatures (K) along the 60°N latitude circle on 11 Jan 1992, and the difference between the two (bottom). Temperature contour interval is 5 K with 240 to 245 K shaded. Difference contour interval is 5 K, with dashed lines indicating negative values.

**Figure 13.** UKMO and NMC potential vorticity (PV) on 11 Jan 1992 at 1450, 840 and 465 K. Layout is as in Fig. 2. Contour interval at 1450 K is  $6 \times 10^{-4} \text{ K m}^2 \text{ kg}^{-1} \text{ s}^{-1}$ , with 30 to  $36 \times 10^{-4} \text{ K m}^2 \text{ kg}^{-1} \text{ s}^{-1}$  shaded; contour interval at 840 K is  $1 \times 10^{-4} \text{ K m}^2 \text{ kg}^{-1} \text{ s}^{-1}$ , with shading between 4 and  $5 \times 10^{-4} \text{ K m}^2 \text{ kg}^{-1} \text{ s}^{-1}$ ; contour interval at 465 K is  $0.05 \times 10^{-4} \text{ K m}^2 \text{ kg}^{-1} \text{ s}^{-1}$ , with shading between 0.25 and  $0.30 \times 10^{-4} \text{ K m}^2 \text{ kg}^{-1} \text{ s}^{-1}$ .

**Figure 14.** As in Fig. 3, but in the SH, and for 15 Aug through 14 Sep 1992. Temperature contour interval is 3 K, with 221 to 224 K shaded. Difference contour interval is 2 K; dashed lines would indicate negative values.

**Figure 15.** As in Fig. 14, but at 46 hPa. Temperature contour interval is 3 K, with 189 to 192 K shaded. Difference contour interval is 0.5 K; dashed lines indicate negative values.

**Figure 16.** As in Fig. 14, but for zonal mean winds ( $\text{m s}^{-1}$ ). Wind contour interval is  $10 \text{ m s}^{-1}$ , with 40 to  $50 \text{ m s}^{-1}$  shaded. Difference contour interval is  $2 \text{ m s}^{-1}$ .

**Figure 17.** As in Fig. 9, but at 68°S. Temperature contour interval is 5 K, with 230 to 235 K shaded. Difference contour interval is 1 K; dashed lines indicate negative values.

**Figure 18.** As in Fig. 17, but for zonal mean wind ( $\text{m s}^{-1}$ ). Wind contour interval is 5  $\text{m s}^{-1}$ , with 45 to 50  $\text{m s}^{-1}$  shaded. Difference contour interval is 2  $\text{m s}^{-1}$ ; dashed lines indicate negative values.

**Figure 19.** As in Fig. 10, but for the SH on 4 Sep 1992. Layout is the same as in Fig. 2, except 0° longitude is at the top of the plots. Temperature contour interval is 5 K. Temperature difference contour interval is 2 K; dashed lines would indicate negative values. Color bars give geopotential height contours.

**Figure 20.** As in Fig. 19, but at 1 hPa. Temperature contour interval is 5 K. Temperature difference contour interval is 4 K; dashed lines indicate negative values. Color bars give geopotential height contours.

**Figure 21.** As in Fig. 12, but around 60°S on 4 Sep 1992. Temperature contour interval is 5 K, with 240 to 245 K shaded. Difference contour interval is 3 K; dashed lines indicate negative values.

**Figure 22.** As in Fig. 13, but for the SH on 4 Sep 1992. Layout is as in Fig. 20. Contours and shading are the same as in Fig. 13, but with negative values of PV in the SH.

**Figure 23.** The difference (NMC - UKMO) between high northern latitude NMC and UKMO temperatures on the 465 K isentropic surface in the lower stratosphere, for December through March, 1991-92 through 1994-95. Labels give the average difference for all days in the period shown.

**Figure 24.** Differences as a function of pressure between UKMO and radiosonde temperatures (solid grey diamonds) and NMC and radiosonde temperatures (open black circles), for all radiosonde measurements with temperatures less than 200 K, and at latitudes between 60° and 76°N, on (a) 14 and 15 Jan 1995, and (b) 28 to 30 Jan 1995.

**Figure 25.** As in Fig. 23, but for southern high latitudes, for May through September, 1992 through 1994.

**Figure 26.** As in Fig. 24, but for  $60^\circ$  and  $76^\circ$ S, and for (a) 11 to 19 Aug 1993, and (b) 11 to 19 Sep 1993.

**Figure 27.** 10 hPa NH UKMO temperatures on 13 Jan 1992. Contour interval is 5 K; shading is from 210 to 215 K; layout is as in Fig. 2.

**Figure 28.** The difference (NMC - UKMO) between NMC and UKMO 10 hPa zonal mean temperatures and zonal mean winds for 15 Dec 1994 through 13 Jan 1995 in the NH. Temperature difference contour interval is 1.5 K; wind difference contour interval is  $2 \text{ m s}^{-1}$ . Dashed lines indicate negative values.

**Figure 29.** 10 hPa S1 I PV on 5 Jul 1993 from (a) UKMO and (b) NMC. Contour interval is  $1 \times 10^{-4} \text{ K m}^2 \text{ kg}^{-1} \text{ s}^{-1}$ ; shading is from  $-7$  to  $-8 \times 10^{-4} \text{ K m}^2 \text{ kg}^{-1} \text{ s}^{-1}$ .

**Table 1.** Summary of rms and average differences between UKMO and radiosonde temperatures, and between NMC and radiosonde temperatures, in the NH lower stratosphere during the 1994-95 winter. Radiosonde measurements between 36 and 54 hPa, and 60° and 76°N are included. Italicized average differences represent biases that are not statistically significant at the 2-*sigma* level.

Dates	Data Type	# sondes	rms $\Delta T$	avg $\Delta T$	# sondes	rms $\Delta T$	avg $\Delta T$
		'1'<2001<	'1'<200 K	'1'<200 K	all '1'	all T	all T
14-16 Dec1994	UKMO	85	2.13	+1.39	591	1.87	+0.57
	NMC	85	1.59	+0.62	591	1.75	-0.18
14-15 Jan 1995	UKMO	165	2.77	+1.31	376	2.50	+1.00
	NMC	165	2.29	+0.76	376	2.20	-0.03
28-30 Jan 1995	UKMO	182	4.52	+3.72	581	3.36	+1.85
	NMC	182	2.13	-1.10	581	2.13	+0.25
14-16 Feb 1995	UKMO	77	3.42	+2.44	677	2.60	+0.54
	NMC	77	2.88	+1.70	677	2.55	-0.21

**Table 2.** Summary of rms and average differences between UKMO and radiosonde temperatures, and between NMC and radiosonde temperatures, in the SH lower stratosphere during the 1993 winter. Radiosonde measurements between 36 and 54 hPa, and 60° and 76°N are included. **Italicized** average differences represent biases that are not statistically significant at the 2-*sigma* level.

Dates	Data Type	# sondes	rms $\Delta T$	avg $\Delta T$	# sondes	rms $\Delta T$	avg $\Delta T$
		T<200 K	T<200K	T<200 K	all T	all T	all T
11-19 May 1993	UKMO	27	1.03	-0.34	178	1.83	-0.73
	NMC	27	.42	+0.81	178	1.55	+0.01
11-19.11.11.11 1993	UKMO	108	.83	-0.47	135	1.90	-0.55
	NMC	108	1.77	+0.27	135	1.79	+0.13
11-19.11.11 1993	UKMO	142	1.43	-0.18	182	2.03	-0.31
	NMC	142	1.69	-10.76	182	1.89	+0.64
11-19 Aug 1993	UKMO	128	1.94	-10.71	162	1.94	-10.70
	NMC	128	2.98	-12.09	162	3.00	-2.06
11-19 Sep 1993	UKMO	130	1.76	-10.83	205	1.88	-10.49
	NMC	130	2.92	-2.4s	205	2.79	-12.05

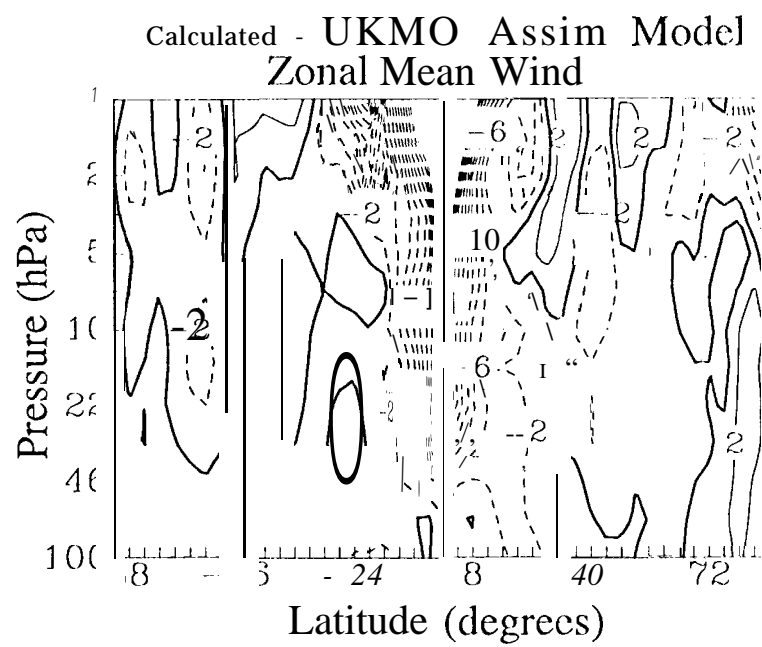
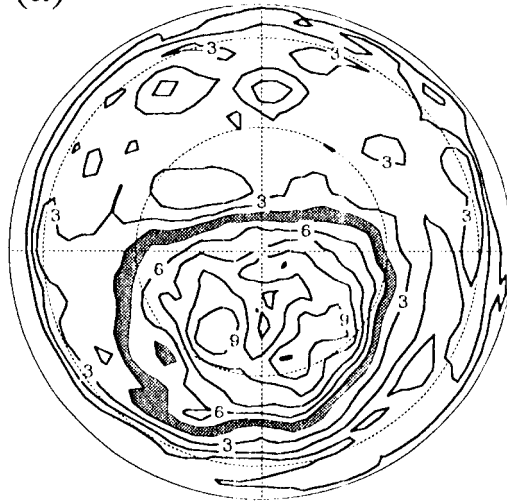


*Fig. 1*

840 K PV, 11 Jan 1992

(a) from Assim winds



(b) from Calc winds

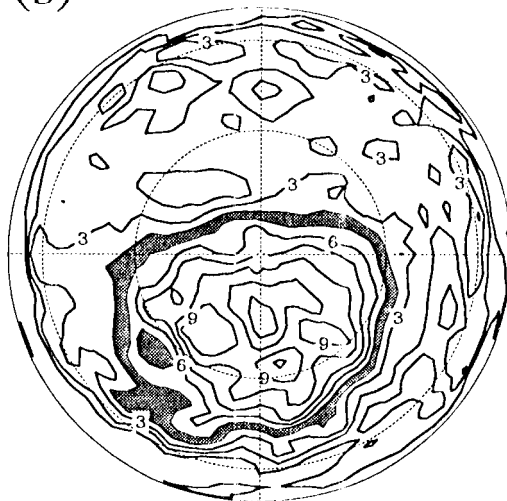


*Fig. 2*



10 hPa zonal mean temperature (K.)

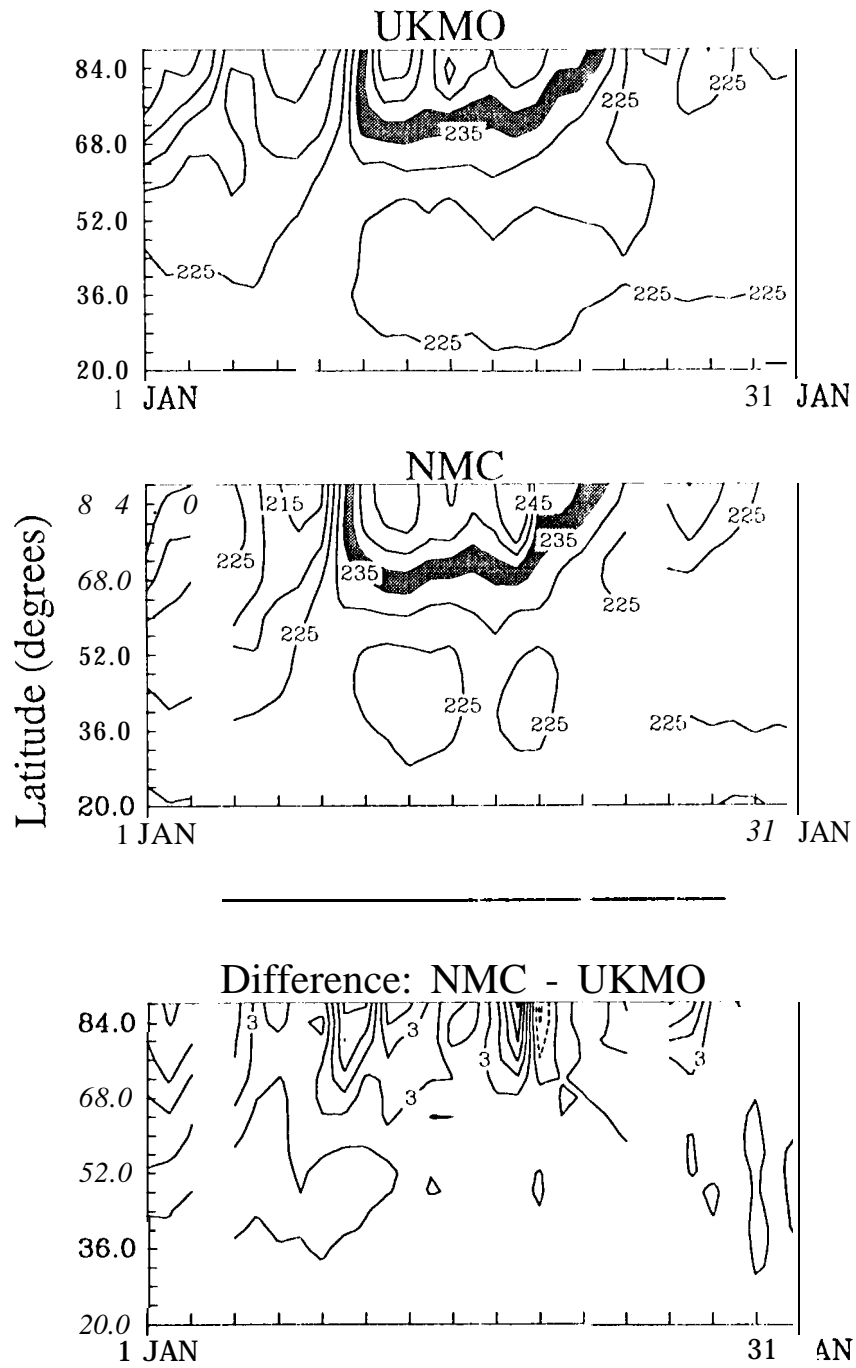


Fig. 3

46 hPa zonal mean temperature (K)

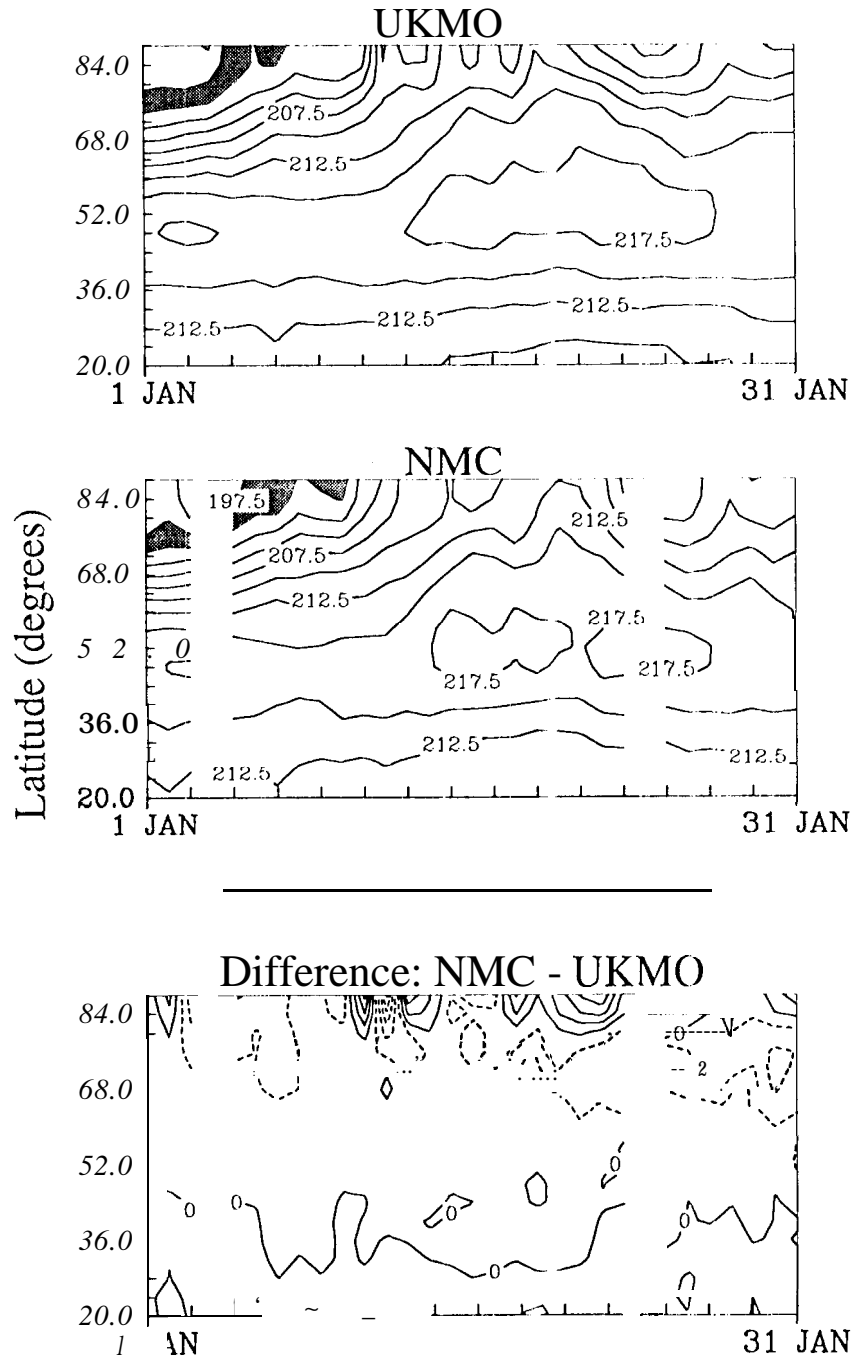
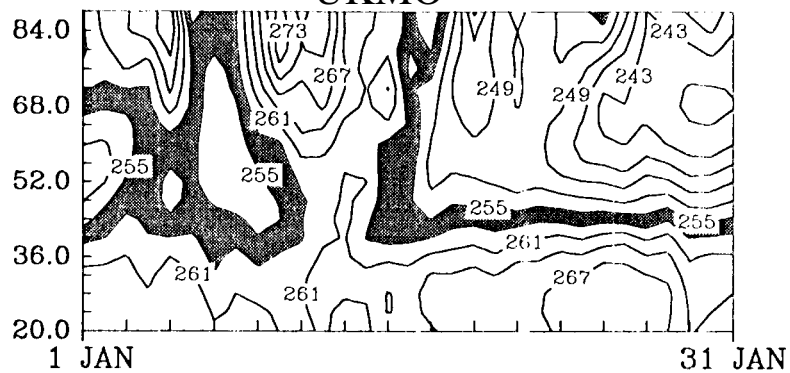


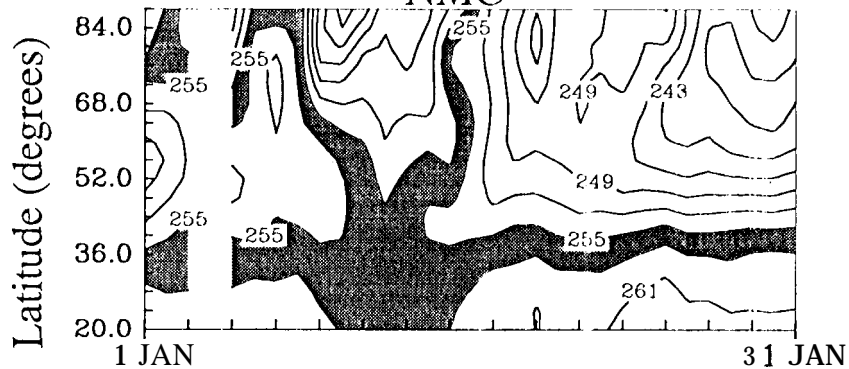
Fig. 4

1 hPa zonal mean temperature (K)

UKMO



NMC



Difference: NMC - UKMO

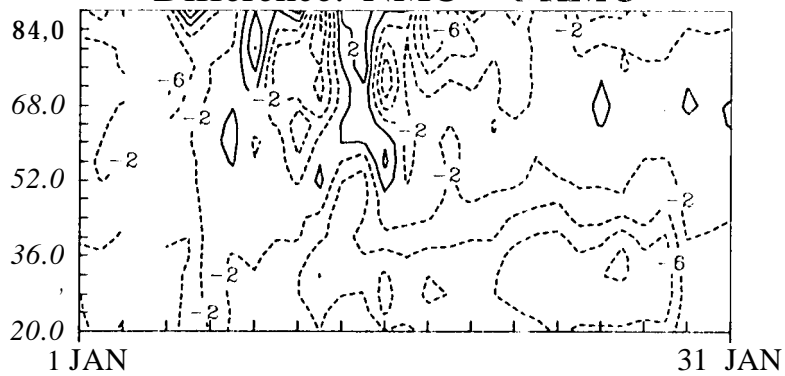


Fig. 5

10 hPa zonal mean wind (m/s)

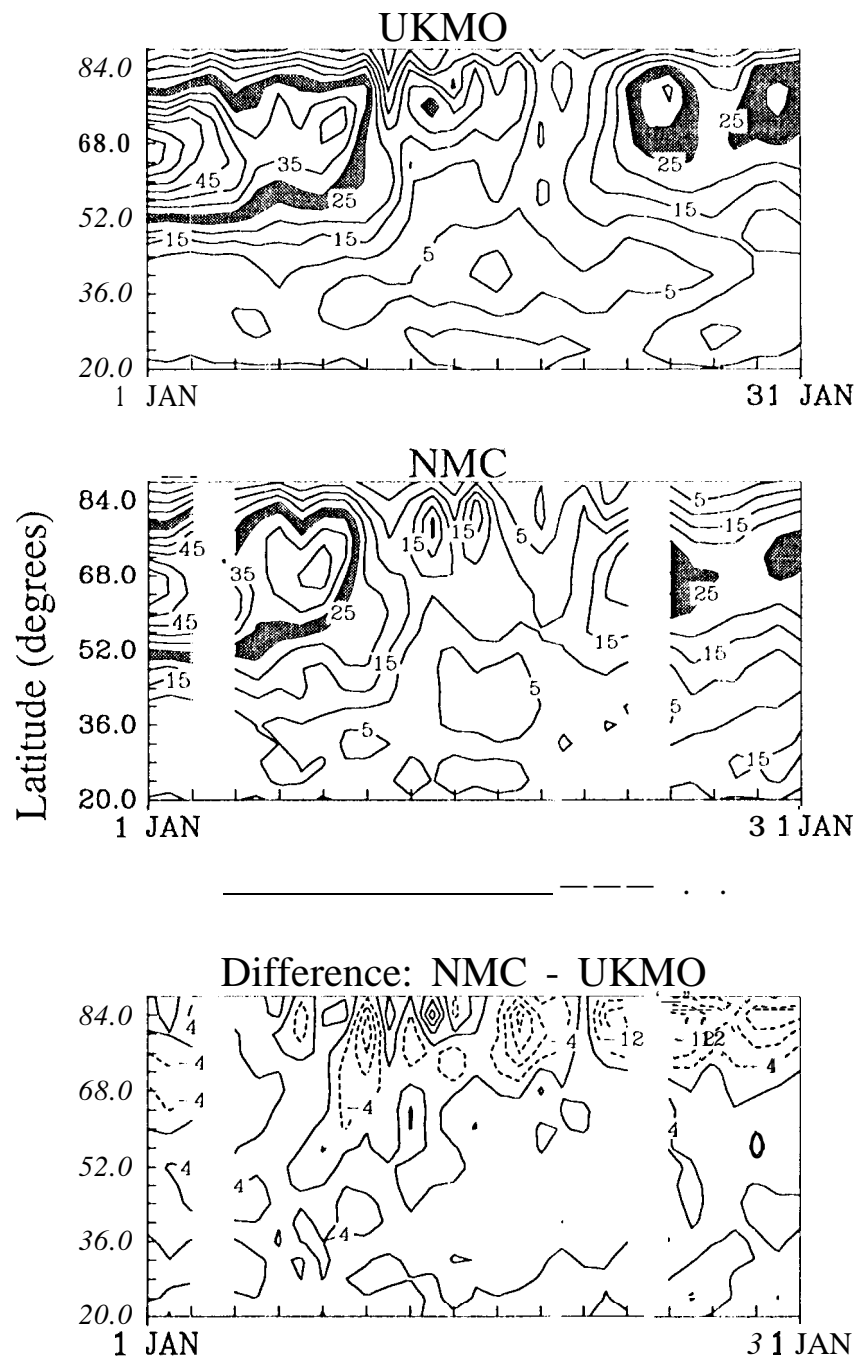


Fig. 6

46 hPa zonal mean wind (m/s)

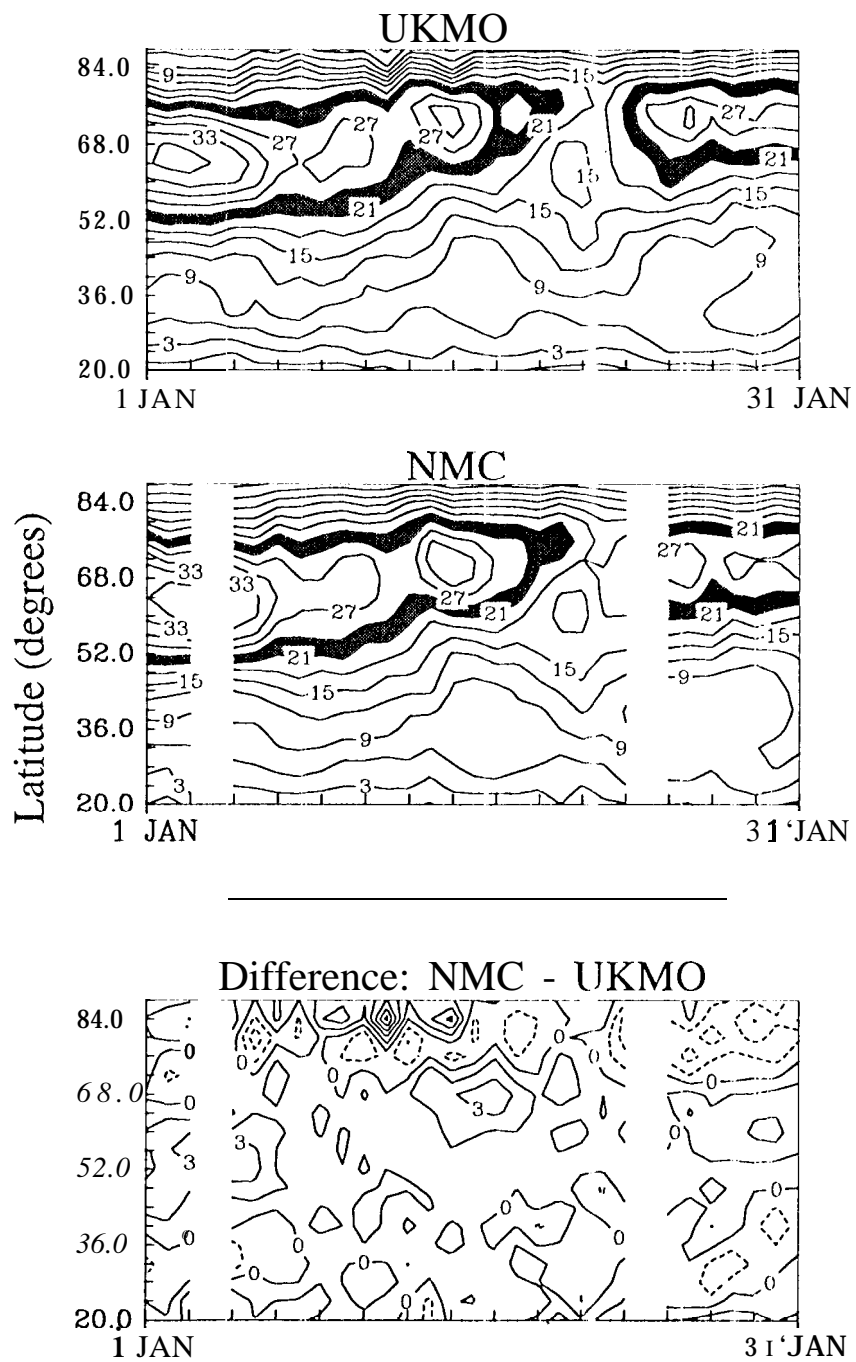


Fig. 7

1 hPa zonal mean wind (m/s)

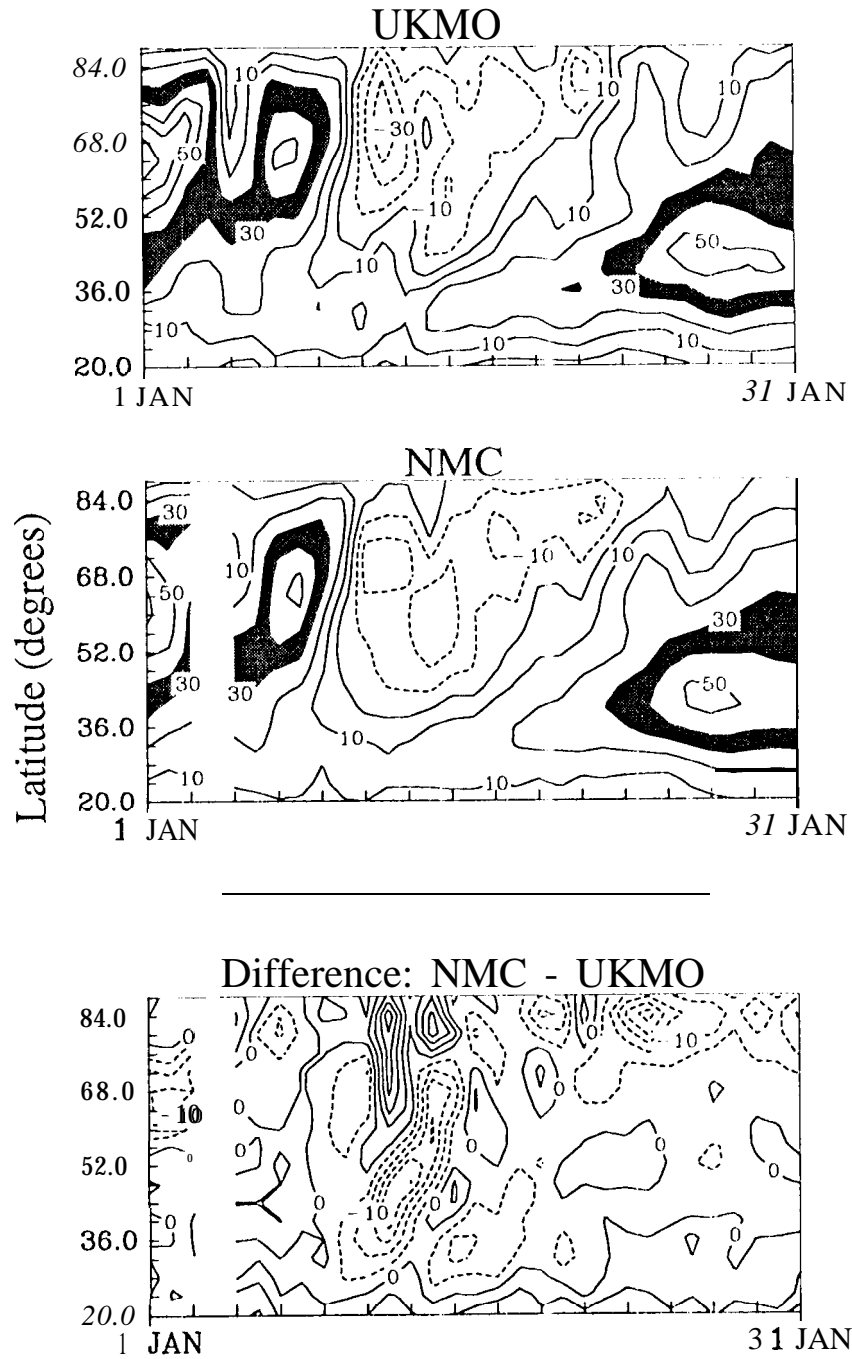
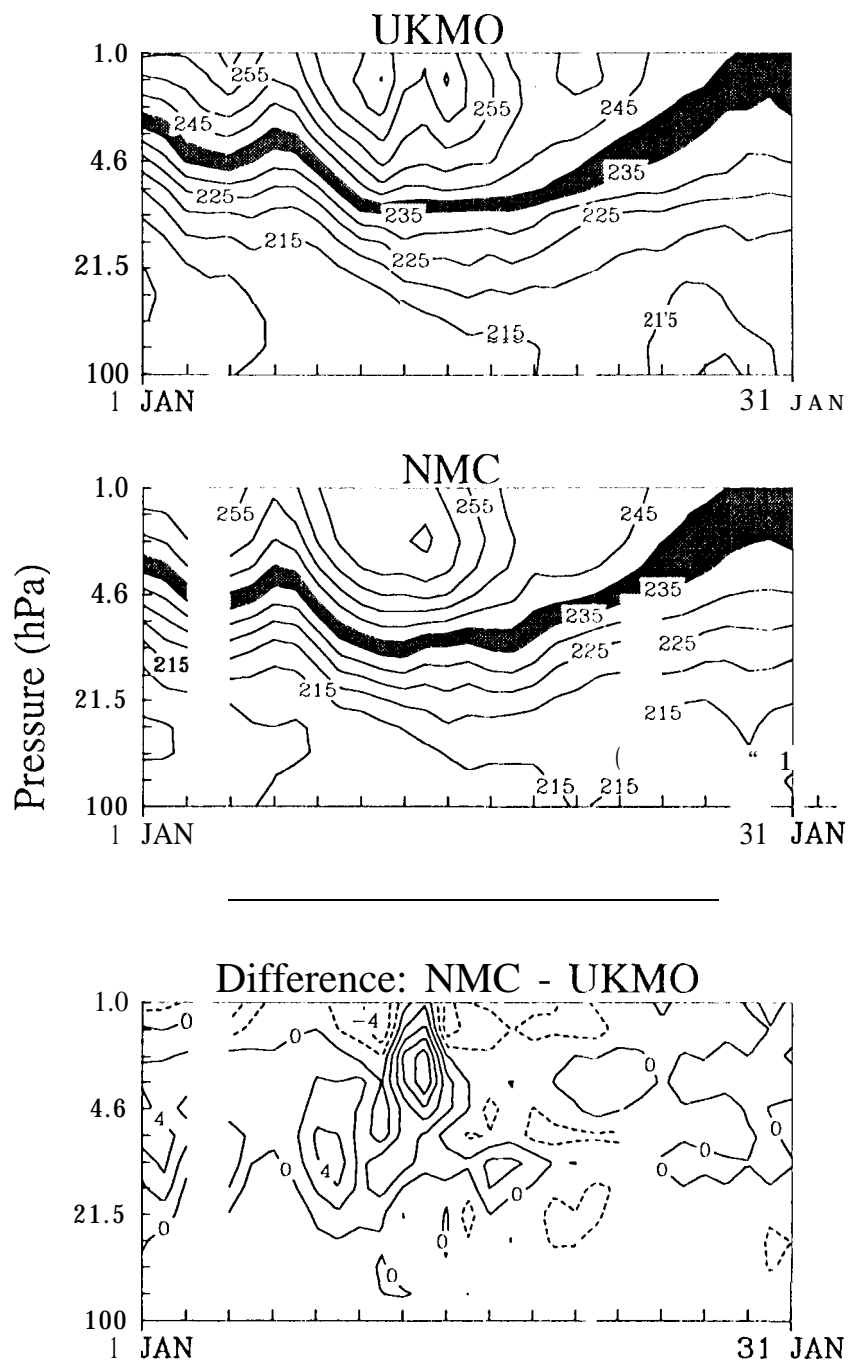


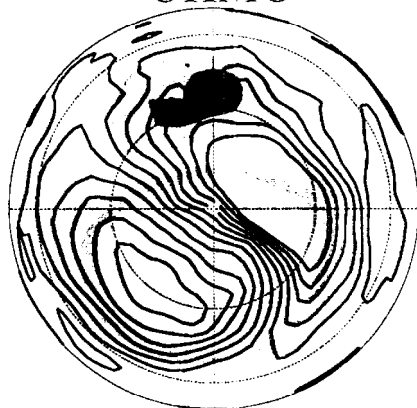
Fig. 8

# 68 N zonal mean temperature (K)

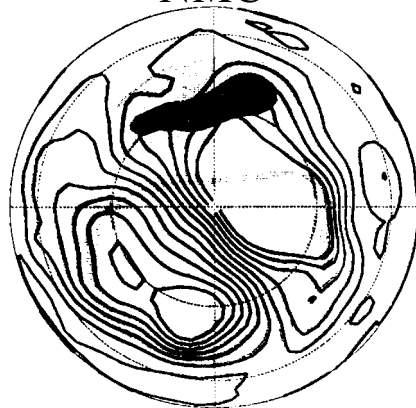


10 hPa geopotential height (km)  
and temperature (K)  
11 Jan 1992

UKMO



NMC



28.8 31.4  
NMC - UKMO



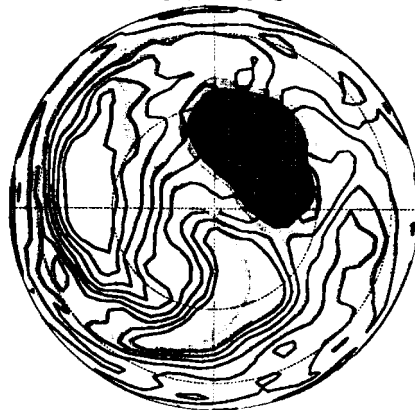
-0.40 0.48

*Fig. 10*

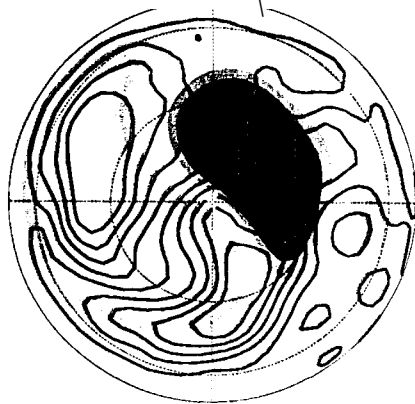


1 hPa geopotential height (km  
and temperature (K)  
11 Jan 1992

UKMO



NMC



45.4 48.4

NMC - UKMO

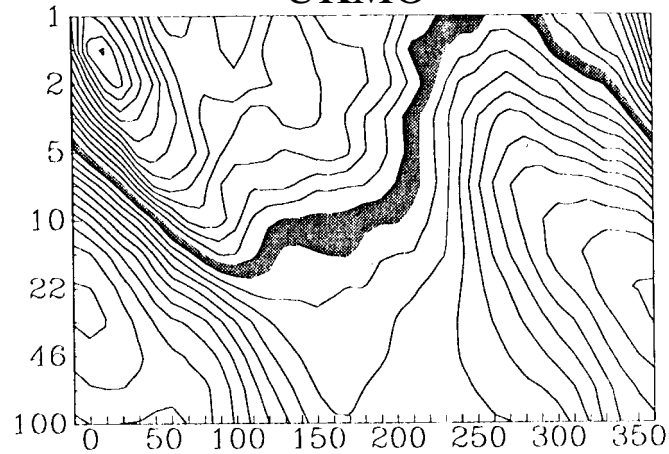


-0.10 0.80

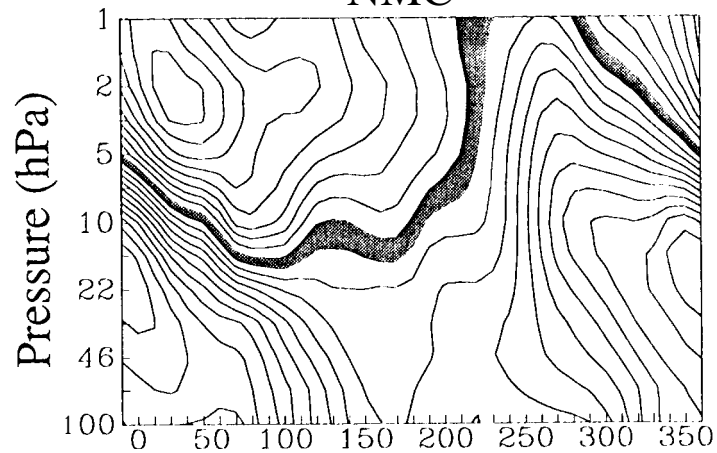
Fig. 11

60 N Temperature (K)  
11 Jan 1992

UKMO



NMC



Difference: NMC - UKMO

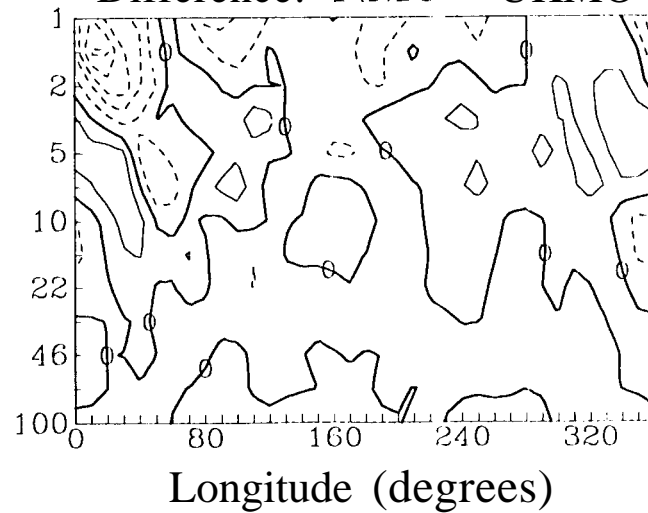


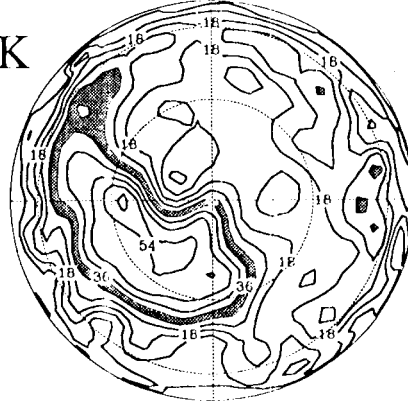
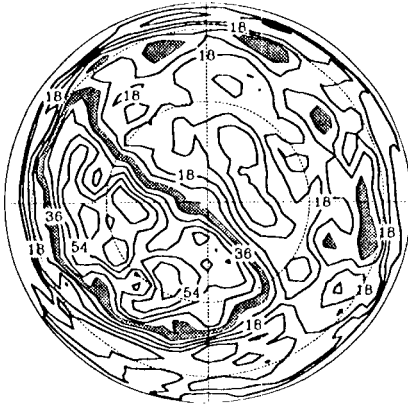
Fig. 12

11 Jan 1992 NH PV

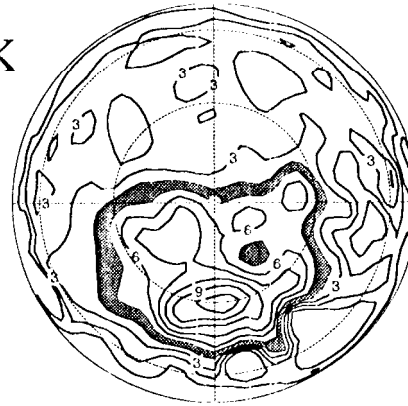
UKMO

NMC

1450 K



840 K



465 K

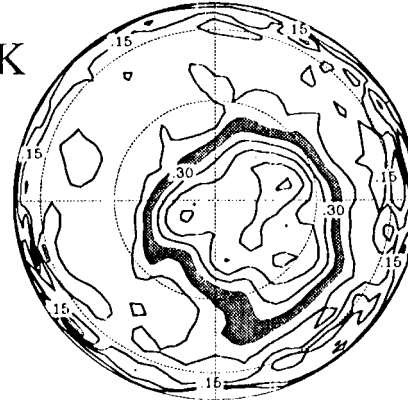
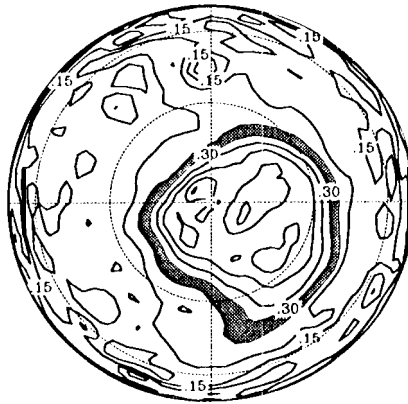
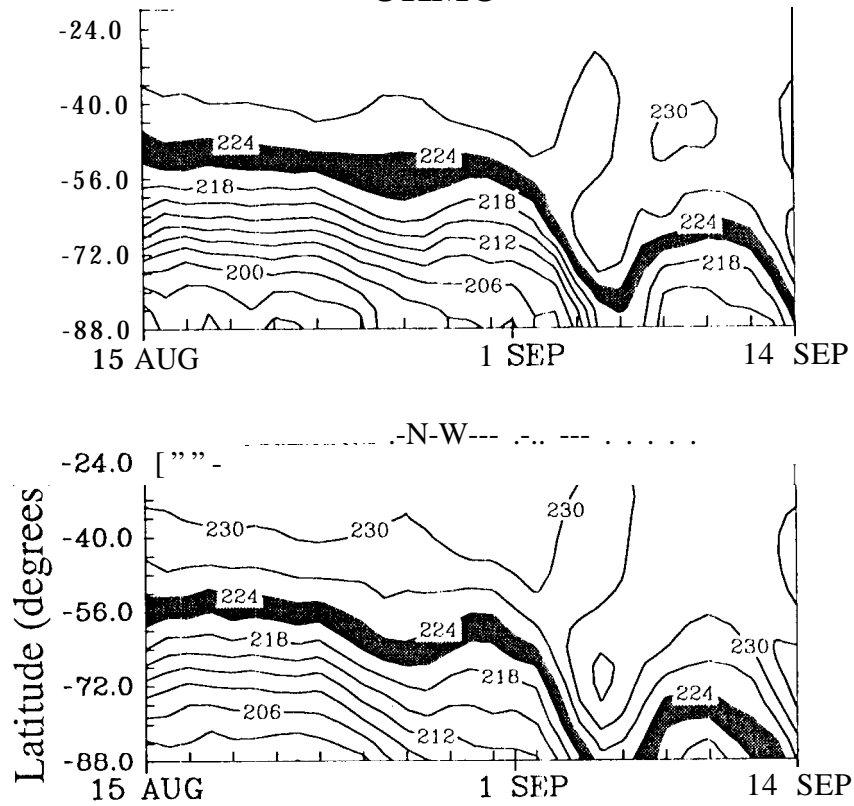


Fig. 13

# 1() hPa zonal mean temperature (K)

UKMO



Difference: NMC - UKMO

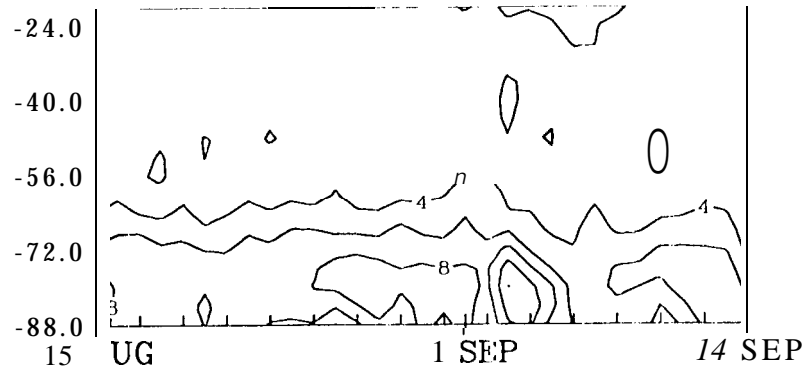


Fig. 14

46 hPa zonal mean temperature (K)

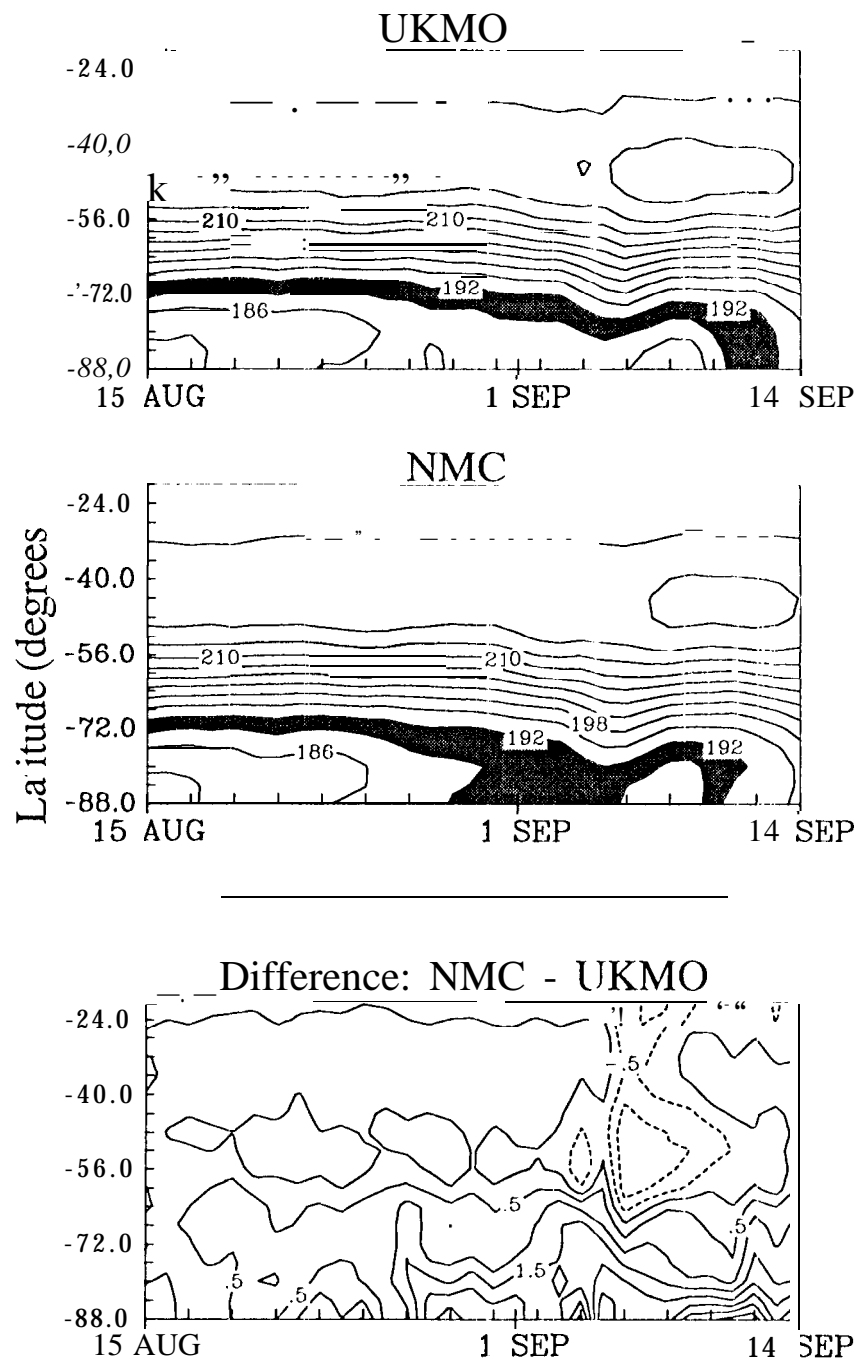


Fig. 15

10 hPa zonal mean wind (m/s)

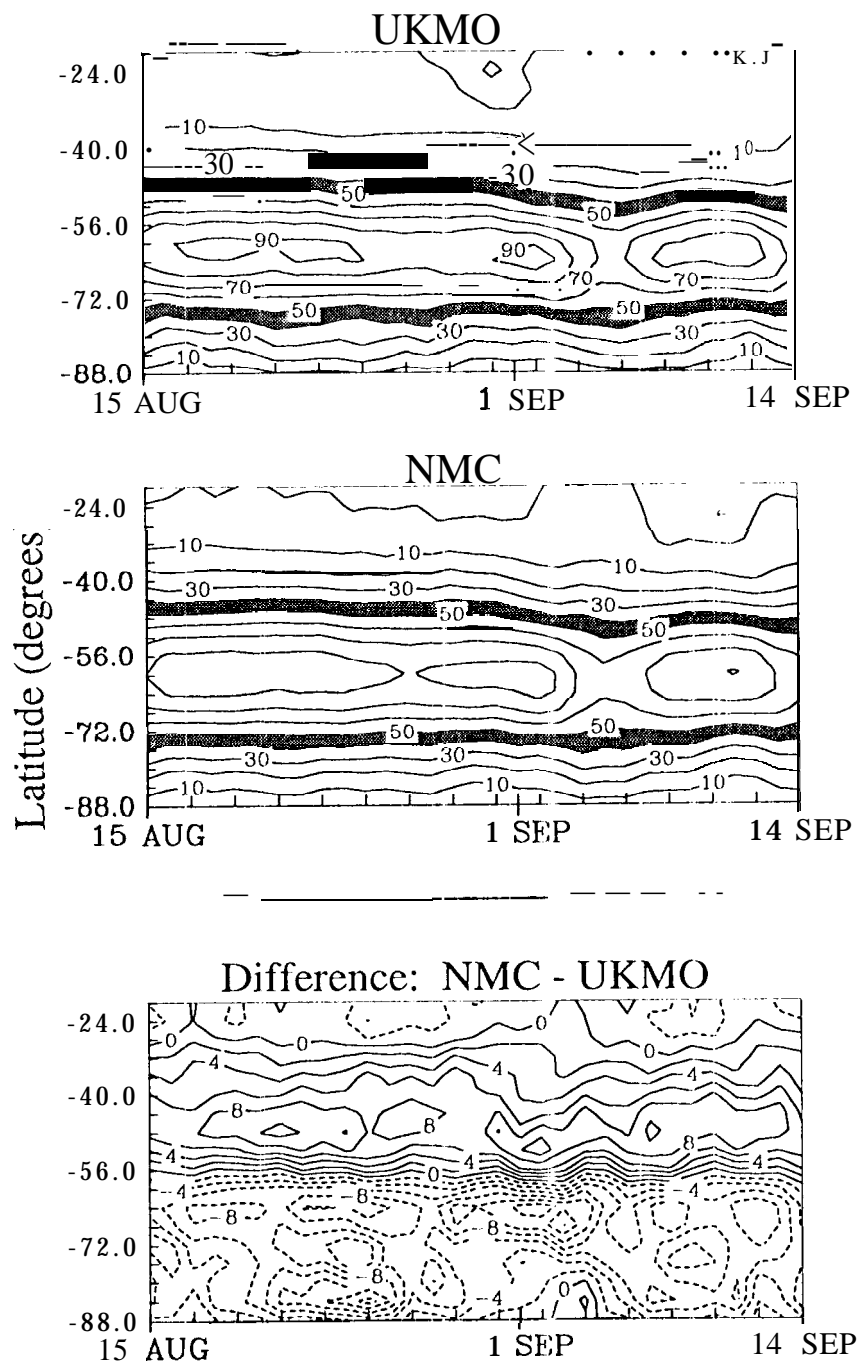


Fig. 16

68 S zonal mean temperature (K)

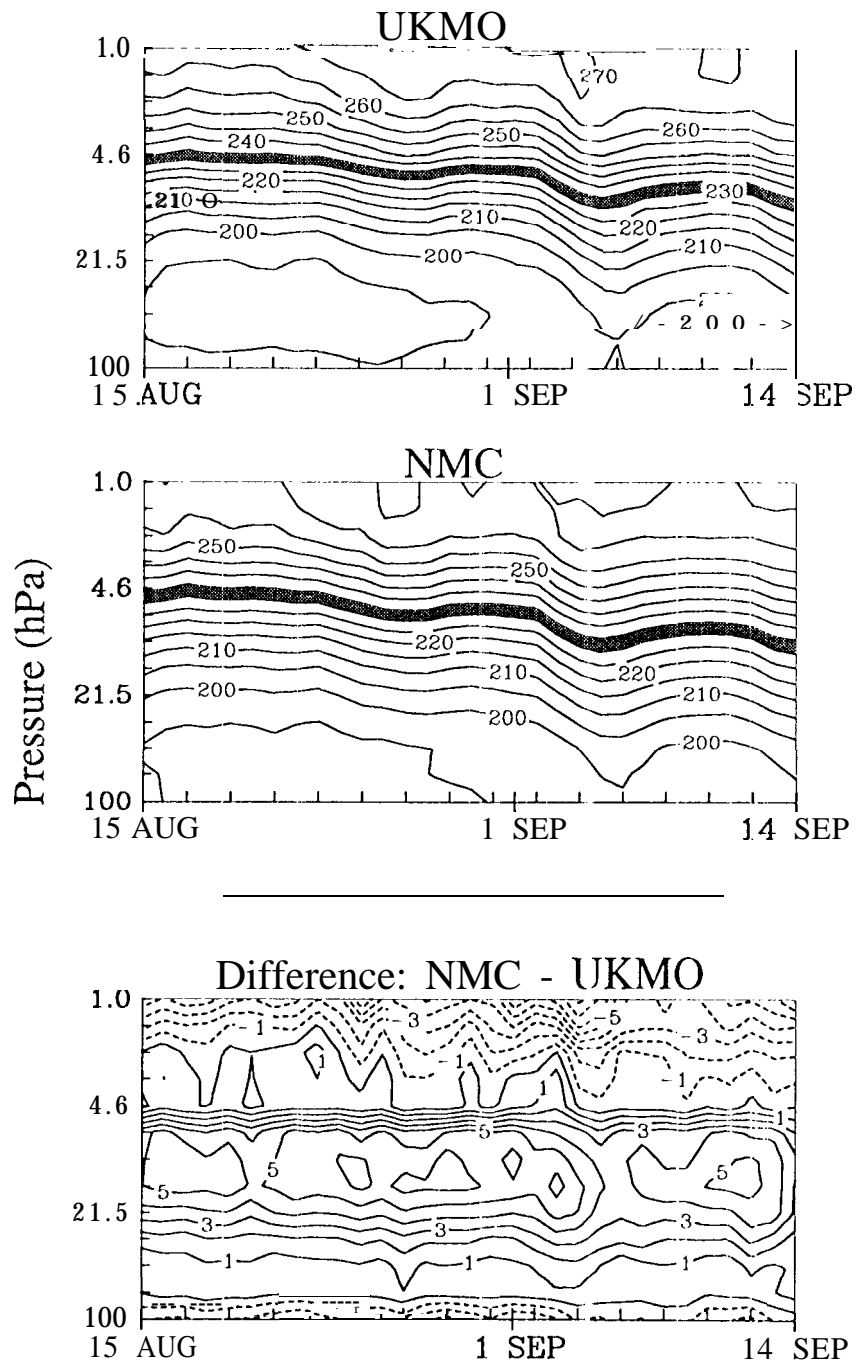


Fig. 17

68 S zonal mean wind (rids)

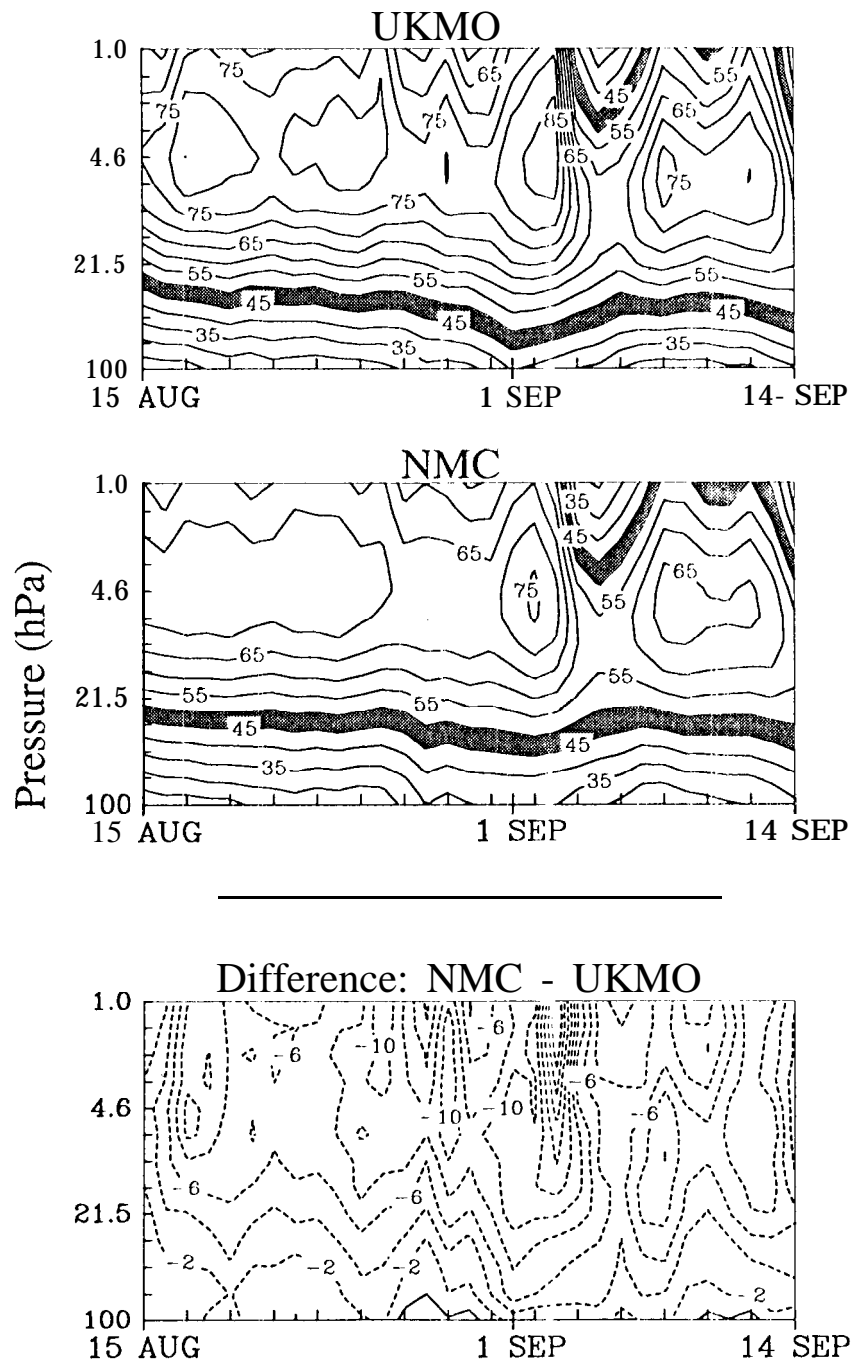


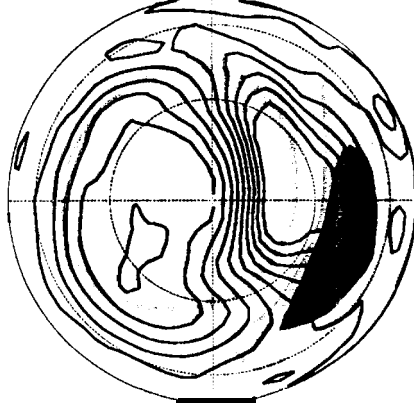
Fig. 18



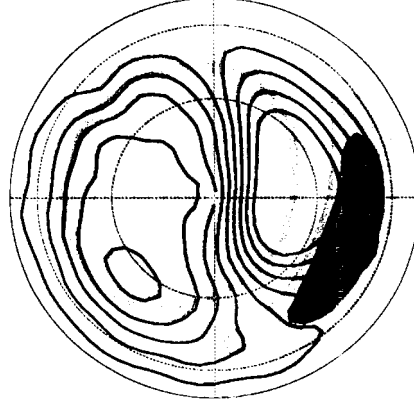
10 hPa geopotential height (km)  
and temperature (K)

4 Sep 1992

UKMO

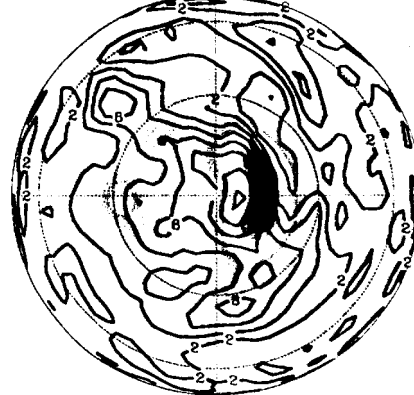


NMC



28,8 31,4

NMC - UKMO

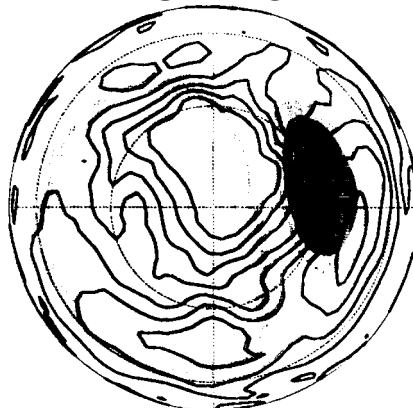


-0.15 0.39

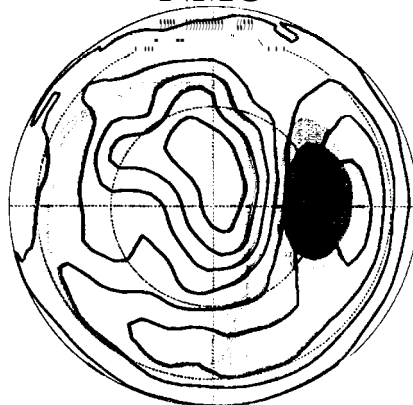
Fig. 19

1 hPa geopotential height (km)  
and temperature (K)  
4 Sep 1992

UKMO



NMC



45.4 48.4

NMC - UKMO

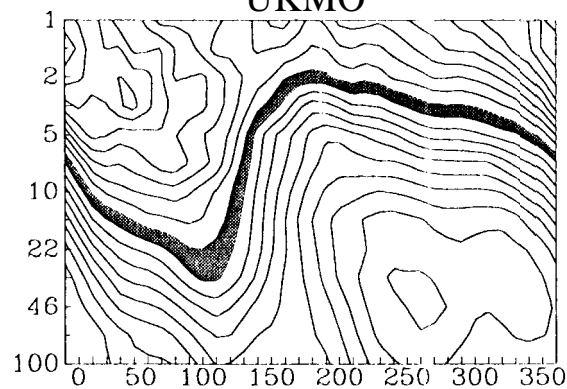


-0.42 0.66

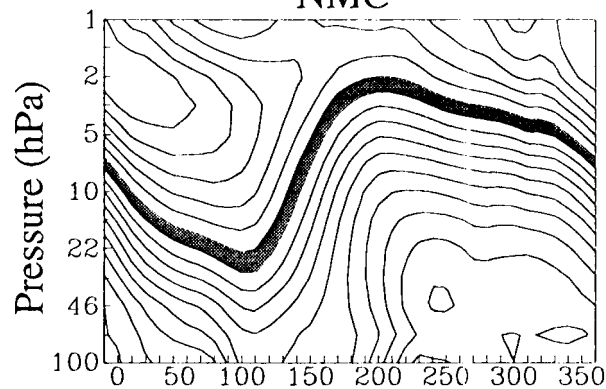
Fig. 20

60 S Temperature (K)  
4 Sep 1992

UKMO



NMC



Difference: NMC - UKMO



Longitude (degrees)

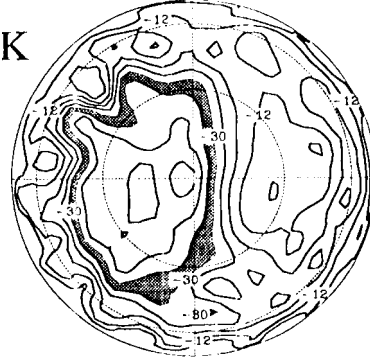
Fig. 21

4 Sep 1992 SH PV

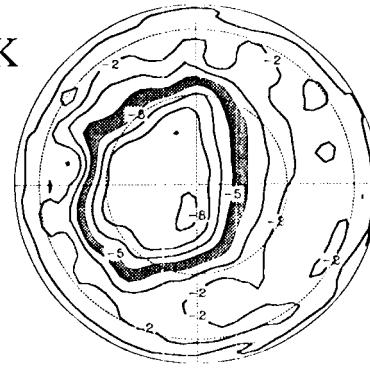
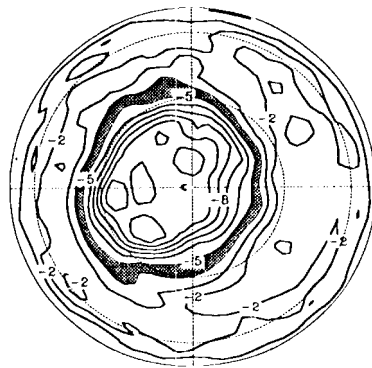
UKMO

NMC

1450 K



840 K



465 K

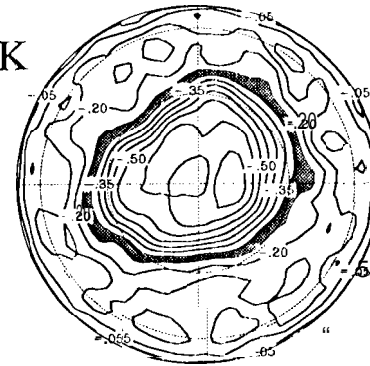
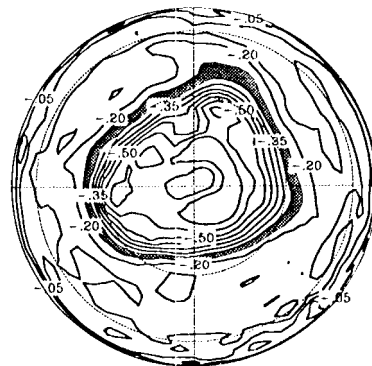


Fig. 22

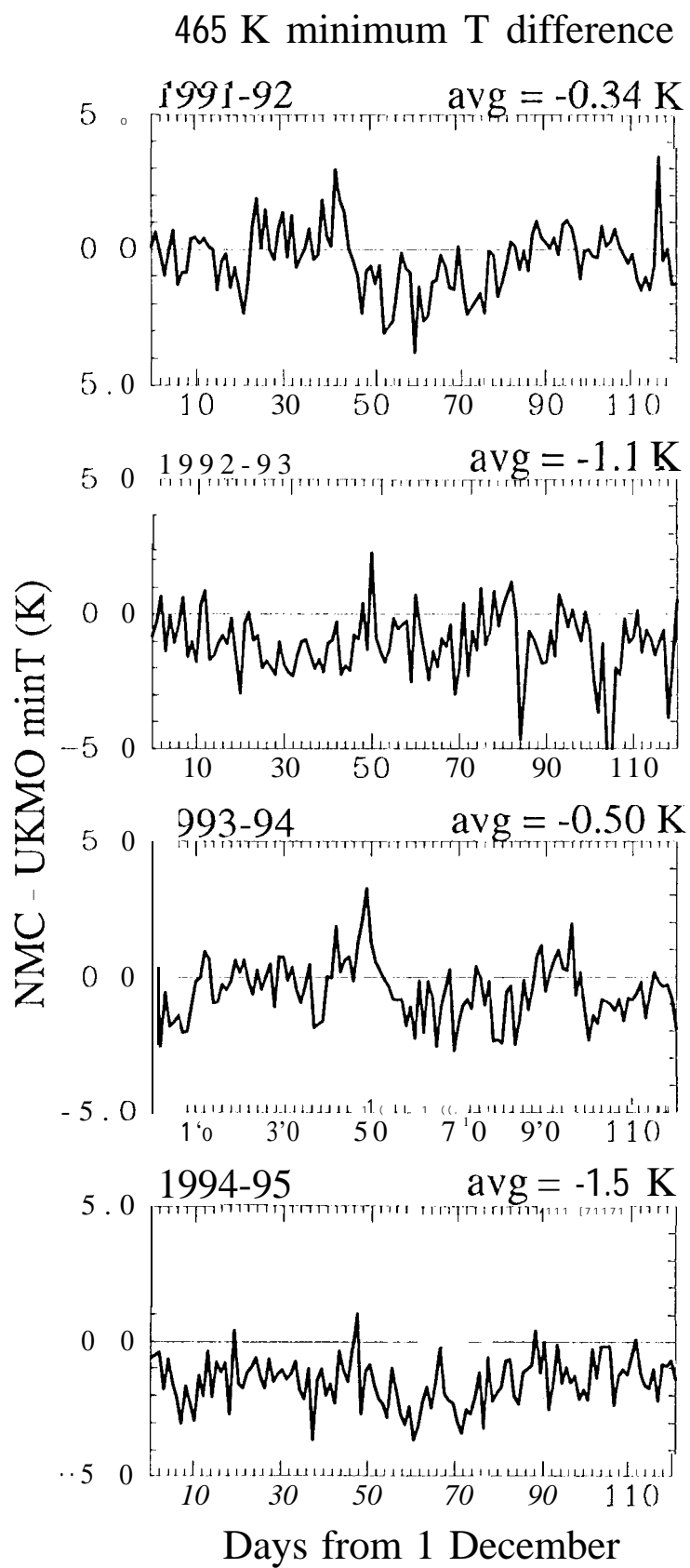


Fig. 23

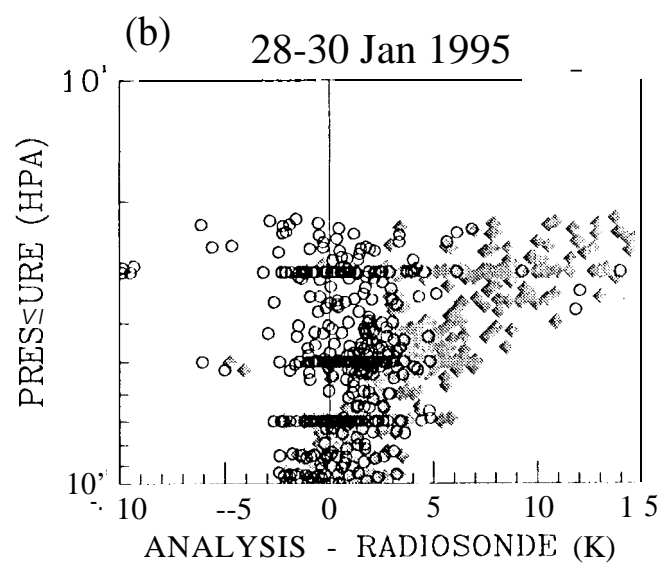
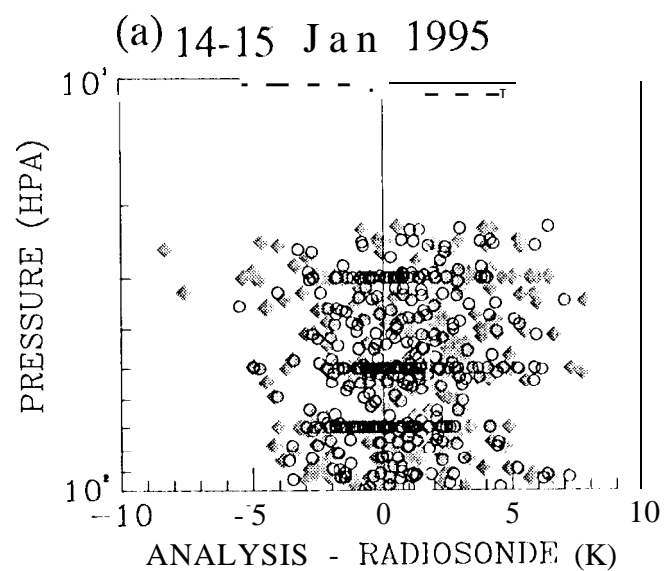


Fig. 24

# 465 K minimum T' difference

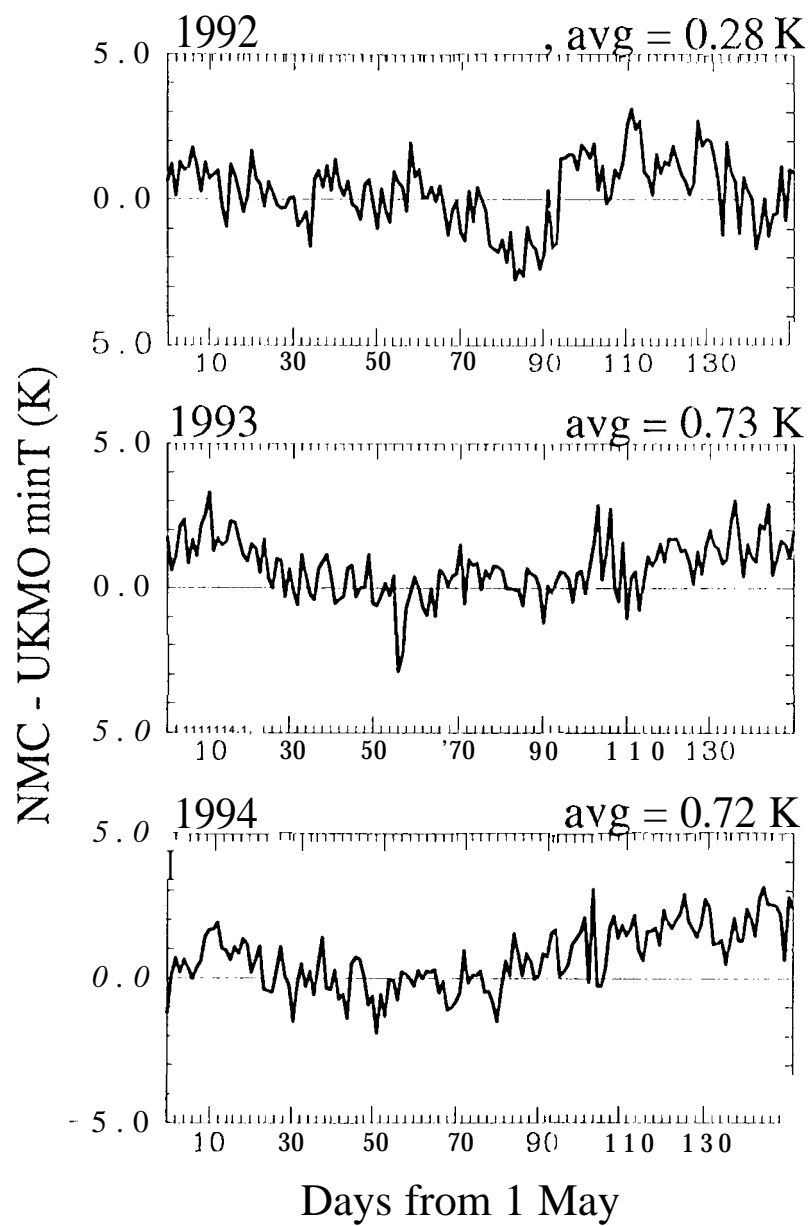


Fig. 25

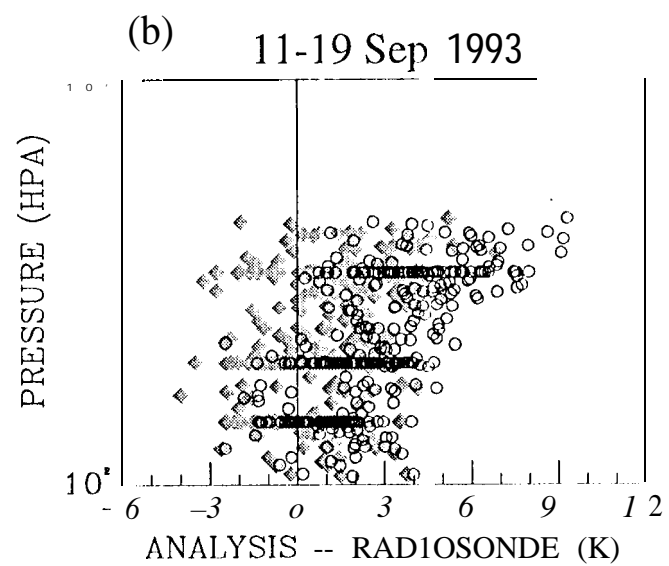
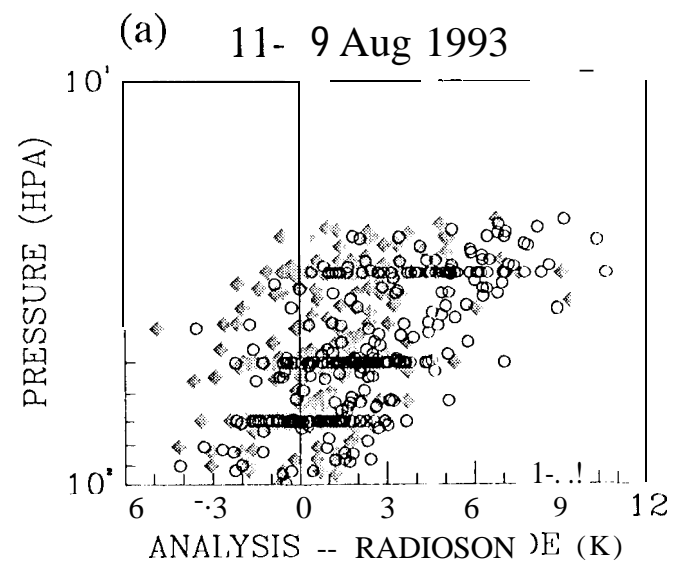


Fig. 26



UKMO 10 hPa T (K)

13 Jan 1992

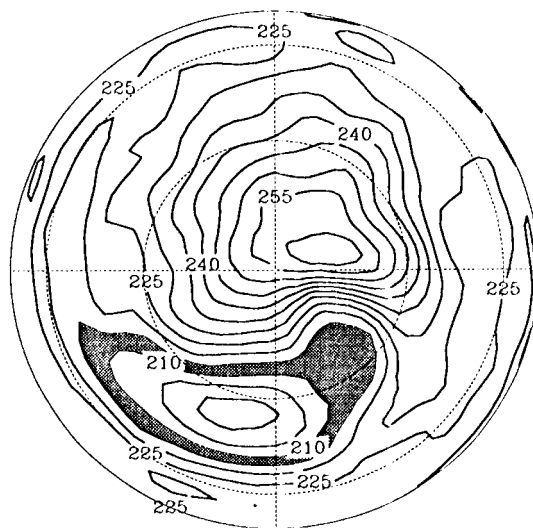


Fig. 27

10 hPa, 1994-95

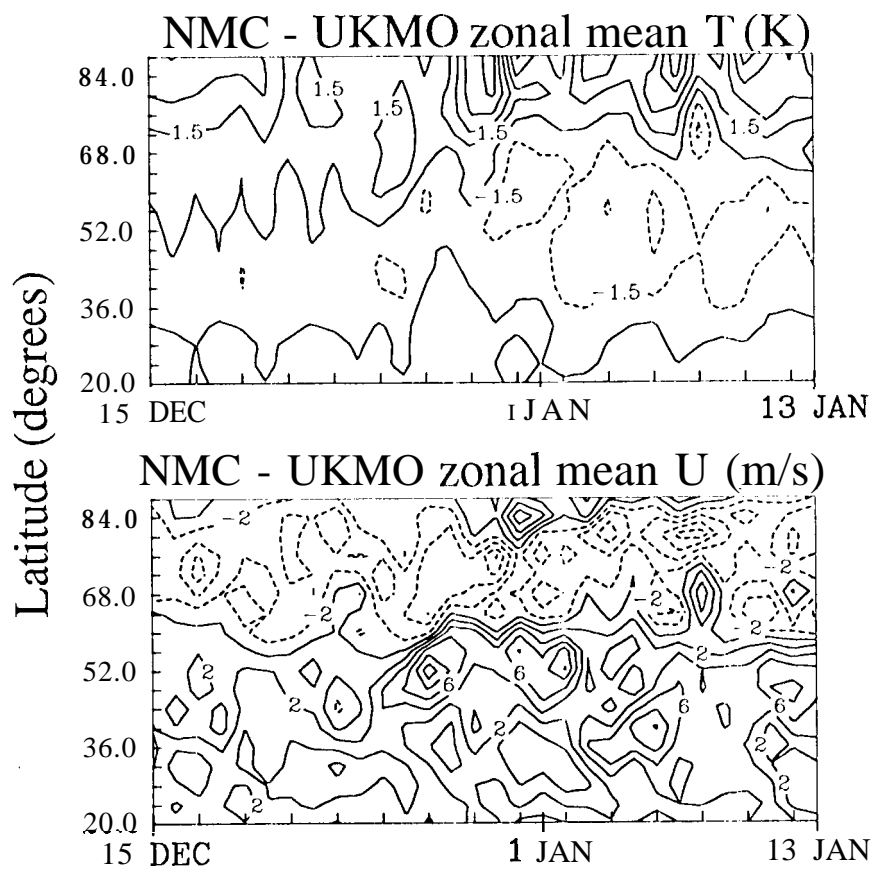
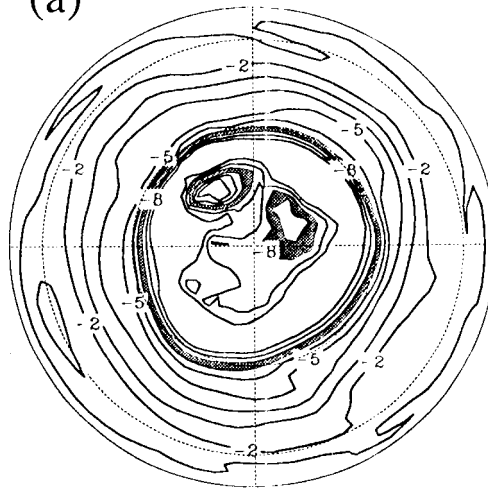


Fig. 28

840 K PV  
5 Jul 1993

(a) UKMO



(b) NMC

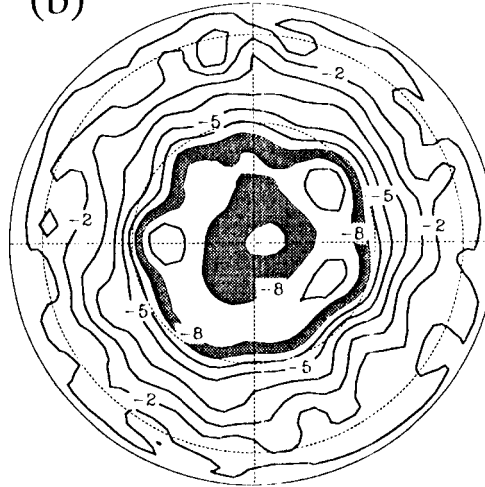


Fig. 29